Data assimilation for morphodynamic model parameter estimation: a hybrid approach.

P.J. Smith, S.L. Dance, N.K. Nichols

August 2009

Abstract

We present a technique for using data assimilation to estimate uncertain model parameters and discuss its application within the context of coastal morphodynamic modelling. A key difficulty in the construction of a data assimilation algorithm is specification of the background error covariances. For parameter estimation, it is particularly important that the cross-covariances between the parameters and the state are given a good a priori specification. We have combined the methods of three dimensional variational data assimilation (3D Var) and the Kalman filter to produce a new hybrid data assimilation scheme that captures the flow dependent nature of the state-parameter cross covariances without explicitly propagating the full system covariance matrix. Here, an idealised two parameter 1D non-linear test model with pseudo-observations is used to demonstrate the method. The results are postive with the scheme able to recover the model parameters to a high level of accuracy. We believe that there is potential for successful application of the methodology to larger, more complex models.

1 Introduction

Data assimilation is a sophisticated mathematical technique for combining observational data with model predictions to 1) produce a model state that most accurately approximates the current and future states of the true system and 2) provide estimates of the model parameters. Data assimilation acts by feeding information from measured observations of the true system into the model, hence producing a model trajectory that more closely follows the true system trajectory and thus improving the ability of the model to predict the future. These observations may be infrequent and need not provide full coverage of the model domain. They may also only be indirectly related to the variables or parameters of interest.

Coastal morphodynamic modelling is challenging; a particular difficulty is that the physical processes that drive morphological change occur on much shorter time-scales than the morphological changes themselves (Masselink and Hughes (2003)). In reality, a model can never completely describe the complex physical processes underlying the behaviour of a morphodynamic system. State of the art models are becoming increasingly sophisticated in an attempt to accurately model coastal morphology (Lesser et al. (2004)) but in practice these models suffer from uncertainity in their initial conditions and parameters. Even with perfect initial data, inaccurate representation of model parameters will lead to the growth of model error and therefore affect the ability of our model to accurately predict the true system state (Ruessink (2005)). A key question in model development is how to estimate these parameters a priori. Generally, parameters are determined theoretically or by adhoc calibration of the model against observations. Various other methods have been developed including downhill simplex optimization (Hill et al. (2003)), genetic algorithm (Knaapen and Hulscher (2003)), and probabilistic approaches (Vrugt et al. (2005), Wüst (2004)). An alternative is to use data assimilation.

While data assimilation has been used in atmospheric and oceanic prediction for some years, it's application within the context of coastal morphodynamic modelling is relatively recent. In a precursor to the current work, Scott and Mason (2007) explored the use of data assimilation for state estimation in estuarine morphodynamic modelling using Morecambe Bay as a study site. A two dimensional depth averaged (2DH) decoupled morphodynamic model of the bay was enhanced by integrating waterline observations derived from SAR (Synthetic Aperture Radar) satellite images (Mason et al. (2001)) using a simple optimal interpolation (OI) assimilation scheme. Despite the known deficiencies of the OI algorithm (see e.g. Lorenc (1981)), the method was shown to improve the ability of the model to predict large scale

changes in bathymetry over a three year period. In an unrelated study, van Dongeren et al. (2008) used a least squares estimator to assimilate multiple, remotely-sensed information sources into the Delft 3D modelling system. This system did not take account of spatial correlations between model variables and thus only updated model variables where there were co-located observations. Nevertheless, the system showed good skill in estimating the nearshore subtidal bathymetry when applied to two data-rich test sites.

The current work is focused on using data assimilation to produce improved morphodynamic model parameter estimates. This can be achieved through *state augmentation*. State augmentation is a conceptually straightforward technique that allows us to estimate and update uncertain model parameters jointly with the model state variables as part of the assimilation process (Jazwinski (1970)). The approach has previously been used in the context of model error or bias estimation (See e.g. Bell et al. (2004), Griffith and Nichols (1996), Griffith and Nichols (2000), Martin et al. (2002), Dee (2005)) and more recently for parameter estimation in biogeochemical models (Trudinger et al. (2008)).

This report builds upon the recent work described in Smith et al. (2008) and Smith et al. (2009) in which the state augmentation method was combined with a three dimensional variational data assimilation (3D Var) scheme and successfullly used to estimate the parameter in an idealised 1D linear model of bedform propagation. A key issue that the previous study highlighted is the importance of the correct specification of the cross covariances between the background state and parameter errors. Conventional 3D Var assumes that the error covariances are stationary; the structure of the background error covariance matrix is specified at the start of the assimilation and kept fixed throughout. It was found that whilst this assumption is sufficient for state estimation, it is insufficient for parameter estimation as it does not provide an adequate representation of these cross-covariances. In order to yield accurate estimates of the true parameters, it is crucial that the state-parameter cross covariances are given a good a priori specification.

Updating the background error covariance matrix at every time step is computationally very expensive, and impracticable when the system of interest is of high dimension. To overcome this problem we have developed a new hybrid data assimilation scheme that gives a flow dependent approximation of the state-parameter cross covariances without explicitly propagating the full system covariance matrix. Here we give details of the formulation of our new method and demonstrate its efficacy using a simplified 1D, two-parameter, non-linear sediment transport model. Although the long term goal is to use data assimilation for parameter estimation in a full morphodynamic assimilation-forecast system applied to some real study sites, the simple model we have chosen for this work provides a framework within which we can develop the technique theoretically and allows us to test our ideas without the obfuscating complexities of a more realistic model. Our results confirm that data assimilation can be used to accurately estimate uncertain model parameters and suggest that the technique of state augmentation could indeed be a useful tool in identifying uncertain morphodynamic model parameters. We believe that the methodology we present has the potential to be transferred not only to larger, more realistic morphodynamic models but also other more general dynamical system models.

This report is organised as follows. In section 2 we explain state augmentation and introduce the augmented system model. In section 3 we give an overview of the 3D Var and the Kalman filter algorithms upon which our new hybrid scheme is based. In section 4 we discuss some of the issues associated with the practical implementation of the state augmentation technique. In section 5 we focus on the specification of the background error covariances and give details of the formulation of our hybrid method. We introduce our simple 1D test model in section 6 and use the results of section 5 to derive estimates for the state-parameter cross covariances in this specific case. The experimental design is described in section 7 followed by the main results. Finally, in section 8 we summarise the conclusions from this work.

2 Data assimilation and state augmentation

The data assimilation methods we present in this section are relevant in many contexts so we describe them for a general system model. The simple model that we have been using to investigate the efficacy of our new scheme will be introduced later in section 6. Our notation is similar to that of Ide et al. (1997).

2.1 Non-linear model system equations

We consider the discrete non-linear time invariant dynamical system model

$$\mathbf{z}_{k+1} = \mathbf{f}(\mathbf{z}_k, \mathbf{p}_k) + \boldsymbol{\varepsilon}_k \qquad k = 0, 1, \ldots, N-1, \tag{2.1}$$

where the vector $\mathbf{z}_k \in \mathbb{R}^m$ is known as the state vector and represents the model state at time t_k, $\mathbf{f}$ is a non-linear operator describing the evolution of the state from time t_k to t_{k+1} and $\mathbf{p}_k \in \mathbb{R}^q$ is a vector of (uncertain) model parameters. Later in this paper we consider the case where the model state vector $\mathbf{z}$ is a 1D vector representing bathymetry or bed height and the operator $\mathbf{f}$ represents the equations describing the evolution of the bed-form over time.

We suppose that we have a set of r observations to assimilate and that these are related to the model state by the equations

$$\mathbf{y}_k = \mathbf{h}(\mathbf{z}_k) + \boldsymbol{\delta}_k, \qquad k = 0, 1, \ldots, N-1. \tag{2.2}$$

Here $\mathbf{y_k} \in \mathbb{R}^r$ is a vector of r observations to assimilate at time t_k and $\mathbf{h} : \mathbb{R}^m \longrightarrow \mathbb{R}^r$ is a nonlinear observation operator that maps from model to observation space. The vector $\boldsymbol{\delta}_k \in \mathbb{R}^r$ represents the observation errors and is commonly interpreted as a white noise sequence (Lewis et al. (2006)). If we have direct measurements but at points that do not coincide with the model grid, $\mathbf{h}$ is simply an interpolation operator that interpolates the model variables from the model grid to the observation locations. Often, the model variables we wish to analyse cannot be observed directly and instead we have observations of another measurable quantity. In this case $\mathbf{h}$ will also include transformations based on physical relationships that convert the model variables to the observations.

We also suppose that we have a *background* state $\mathbf{z}_0^b \in \mathbb{R}^m$, with error $\boldsymbol{\varepsilon}_0^b \in \mathbb{R}^m$, that represents an *a priori* estimate of the true initial system state $\mathbf{z}_0$. This is a best guess estimate obtained (for example) from a previous assimilation run or a recent bathymetric survey.

The aim of data assimilation is to combine the measured observations $\mathbf{y}$ with the model predictions $\mathbf{z}^b$ in order to derive an updated model state that most accurately describes the true state of the system $\mathbf{z}^t$. This optimal estimate is called the *analysis* and is denoted $\mathbf{z}^a$.

2.2 State augmentation

Data assimilation is most commonly used for 'state estimation'; estimating model variables whilst keeping the model parameters fixed. However, by employing the technique of state augmentation (also known as joint estimation), it is also possible to use data assimilation to estimate uncertain model parameters.

In theory state augmentation can be applied with any of the standard data assimilation methods. The model state vector is augmented with a vector containing the parameters we wish to estimate, the equations governing the evolution of the model state are combined with the equations describing the evolution of these parameters and the chosen assimilation algorithm is simply applied to this new augmented system in the usual way. Navon (1997) and Evensen et al. (1998) review the use of the technique in the context of 4D Var. Yang and Hamrick (2003) use a related scheme to recover parameters for cohesive sediment modelling. State augmentation has also been applied with the Kalman filter; Martin (2000) uses the method for model bias estimation and Trudinger et al. (2008) combine the technique with the extended and ensemble Kalman filters for parameter estimation in biogeochemical models.

2.2.1 The augmented system

The model (2.1) depends on parameters whose values are imprecisely known. Sediment transport models, for example, are typically based on empirical formulae that use various parameterizations to characterise the physical properties of the sediment flux. We use the vector $\mathbf{p} \in \mathbb{R}^q$ to represent these parameters, where q is the number of unknowns. We assume that they are time-invariant, that is, they are not altered by the forecast model from one time step to the next. The parameter vector $\mathbf{p}$ is therefore constant and the model for the evolution of the parameters can be written as

$$\mathbf{p}_{k+1} = \mathbf{p}_k. \tag{2.3}$$

Combining (2.3) with the model for the evolution of the state (2.1) we can write the equivalent augmented

system model as

$$\mathbf{w}_{k+1} = \tilde{\mathbf{f}}(\mathbf{w}_k), \tag{2.4}$$

where

$$\mathbf{w} = \begin{pmatrix} \mathbf{z} \\ \mathbf{p} \end{pmatrix} \in \mathbb{R}^{m+q}, \tag{2.5}$$

is the *augmented state vector*, and

$$\tilde{\mathbf{f}}(\mathbf{w}_k) = \begin{pmatrix} \mathbf{f}(\mathbf{z}_k, \mathbf{p}_k) \\ \mathbf{p}_k \end{pmatrix} \in \mathbb{R}^{m+q}. \tag{2.6}$$

We rewrite the equation for the observations (2.2) in terms of the augmented state vector as

$$\mathbf{y}_k = \tilde{\mathbf{h}}(\mathbf{w}_k) + \boldsymbol{\delta}_k, \tag{2.7}$$

where $\tilde{\mathbf{h}} : \mathbb{R}^{m+q} \longrightarrow \mathbb{R}^r$, and

$$\tilde{\mathbf{h}}(\mathbf{w}) = \tilde{\mathbf{h}} \begin{pmatrix} \mathbf{z} \\ \mathbf{p} \end{pmatrix} = \mathbf{h}(\mathbf{z}). \tag{2.8}$$

Our aim is now to combine the observations $\mathbf{y}$ with the augmented model predictions $\mathbf{w}^b$ to produce an analysis state $\mathbf{w}^a$ that most accurately describes the true augmented system state $\mathbf{w}^t$. Note that our initial background state $\mathbf{w}_0^b \in \mathbb{R}^{m+q}$, must now include prior estimates of both the initial system state $\mathbf{z}_0$ and parameters $\mathbf{p}_0$. In addition to the updated state estimate, the analysis $\mathbf{w}^a$ will also include updated estimates of the model parameters.

3 Data assimilation methods

A wide variety of data assimilation schemes exist (e.g. Kalnay (2003), Lewis et al. (2006)). In this study we combine the methods of three dimensional variational data assimilation (3D Var) and the Kalman filter to produce a new hybrid scheme. Sections (3.1) and (3.2) give a brief overview of these two methods. Although we discuss their formulation specifically in terms of our augmented system we note that both schemes were orginally developed for basic state estimation. The equations are equivalent can be derived by simply omitting the parameter vector from our descriptions.

3.1 Three dimensional variational assimilation

The 3D Var method is so called because it resolves the three spatial dimensions but does not account for the fourth dimension - time. Instead 3D Var schemes are designed to produce an analysis at a single time. Typically, in applications such as NWP, observations are not taken simultaneously but are collected across a given time window. 3D Var schemes assume that the state does not evolve significantly within this period and treats all observations as if they had been taken at the same time and assimilating them simultaneously. The analysis time is usually taken as the midpoint of the observation time window. If a 3D Var scheme is applied cyclically (as is done in this work) it can be regarded as a sequential data assimilation method. With sequential assimilation the model is evolved one step at a time; each time a new set of observations becomes available a new analysis is produced giving an updated estimate of the current system state. The model is then forecast forward to the time of the next observations, using the analysis as the initial state, and the assimilation process is repeated.

The 3D Var method (e.g. Courtier et al. (1998)) is based on a maximum a posteriori estimate approach and derives the analysis by seeking a state that minimises a cost function measuring the misfit between the model state $\mathbf{w}$ and the background state $\mathbf{w}^b$ and the observations $\mathbf{y}$,

$$J(\mathbf{w}) = (\mathbf{w} - \mathbf{w}^b)^{\mathbf{T}} \tilde{\mathbf{B}}^{-1} (\mathbf{w} - \mathbf{w}^b) + (\mathbf{y} - \tilde{\mathbf{h}}(\mathbf{w}))^{\mathbf{T}} \mathbf{R}^{-\mathbf{1}} (\mathbf{y} - \tilde{\mathbf{h}}(\mathbf{w})). \tag{3.1}$$

The matrices $\tilde{\mathbf{B}} \in \mathbb{R}^{(m+q)\times(m+q)}$ and $\mathbf{R} \in \mathbb{R}^{r\times r}$ are the covariance matrices of the background and observation errors. If we assume that these errors are unbiased, we can define

$$\tilde{\mathbf{B}} = E\left(\boldsymbol{\varepsilon}_b \boldsymbol{\varepsilon}_b^T\right) \quad \text{and} \quad \mathbf{R} = E\left(\boldsymbol{\delta}\,\boldsymbol{\delta}^T\right), \tag{3.2}$$

where $\boldsymbol{\varepsilon}_b = \mathbf{w}^b - \mathbf{w}^t$ and $\boldsymbol{\delta} = \mathbf{y} - \tilde{\mathbf{h}}(\mathbf{w}^t)$.

These matrices represent the uncertainties of the background and observations and determine the relative weighting of $\mathbf{w}^b$ and $\mathbf{y}$ in the analysis. If it is assumed that the background errors are small relative to the observation errors then the analysis will be close to the background state. Conversely, if it is assumed that the background errors are relatively large the analysis will lie closer to the observations.

The analysis $\mathbf{w}^a$ is found using the gradient of the cost function with respect to $\mathbf{w}$. The 3D Var method does this numerically using a gradient descent algorithm to iterate to the minimising solution (Gill et al. (1981)).

The crucial difference between standard 3D Var and other schemes such as 4D Var and the Kalman filter is that the error covariance matrices are not evolved (implicitly or explicitly) by the 3D Var algorithm. The background error covariance matrix has a fundamental impact on the quality of the analysis. Its prescription is therefore generally considered to be one of the most difficult and important parts in the construction of a data assimilation scheme. The 3D Var method approximates this matrix once at the start of the assimilation window and then holds it fixed throughout, as if the forecast errors were statistically stationary. It is therefore vital that it is given a good a priori specification.

3D Var is a robust and well established method that has many advantages, such as ease of implementation (no model adjoints required); computational robustness (given reasonably specified covariances) and computational efficiency.

3.2 The Kalman filter

The Kalman filter is also a sequential method. It was developed by Kalman (1960) and Kalman and Bucy (1961) and initially used in engineering applications. For a linear system, the Kalman filter algorithm produces an analysis that is (given the available observations and under certain statistical assumptions) statistically optimal in the sense that it the minimum mean square error, or minimum variance, estimate (Barnett and Cameron (1990), Jazwinski (1970)).

The main distinctions between the Kalman filter and 3D Var is that the error covariances are evolved explicitly according to the model dynamics and the analysis is calculated directly. Instead of assuming that the background error covariance matrix is fixed, the Kalman filter forecasts $\tilde{\mathbf{B}}$ forward, using knowledge of the quality of the current analysis to specify the covariances for the next assimilation step. This allows information from all previously assimilated observations to be taken into account, giving much greater observational impact.

Below we present the Kalman filter algorithm for a discrete linear time-invariant model. We are assuming a perfect model (i.e. zero model error) but note that this is not a necessary assumption since the Kalman filter does allow for the inclusion of random model error (see for example, Martin et al. (1999)). Notation is as above except: the background state vector $\mathbf{w}^b$ is replaced by the forecast vector $\mathbf{w}^f$ to denote the fact that the background is now a forecast; the background error covariance matrix $\tilde{\mathbf{B}}$ is replaced by $\mathbf{P}^f$; and we introduce a new matrix $\mathbf{P}^a$ representing the analysis error covariance.

3.2.1 The Kalman filter predict and update equations

For a perfect, discrete linear time invariant dynamical system model

$$\mathbf{w}_{k+1} = \mathbf{F}\mathbf{w}_k \qquad k = 0, 1, \ldots, N-1,$$

with observations linearly related to the state by the equations

$$\mathbf{y}_k = \tilde{\mathbf{H}}_k \mathbf{z}_k + \boldsymbol{\delta}_k. \tag{3.3}$$

where $\mathbf{F}$ is a constant, non-singular matrix describing the dynamic evolution of the state from time t_k to time t_{k+1} and $\tilde{\mathbf{H}}_k \in \mathbb{R}^{r\times(m+q)}$,

the Kalman filter consists of the following steps:

State forecast:

$$\mathbf{w}^f_{k+1} = \mathbf{F}\mathbf{w}^a_k \tag{3.4}$$

Error covariance forecast:

$$\mathbf{P}^f_{k+1} = \mathbf{F}\mathbf{P}^a_k\mathbf{F}^T \tag{3.5}$$

Kalman gain:

$$\tilde{\mathbf{K}}_{k+1} = \mathbf{P}^f_{k+1}\tilde{\mathbf{H}}^T_{k+1}(\tilde{\mathbf{H}}_{k+1}\mathbf{P}^f_{k+1}\tilde{\mathbf{H}}^T_{k+1} + \mathbf{R}_{k+1})^{-1} \tag{3.6}$$

Analysis:

$$\mathbf{w}^a_{k+1} = \mathbf{w}^f_{k+1} + \tilde{\mathbf{K}}_{k+1}(\mathbf{y}_{k+1} - \tilde{\mathbf{H}}_{k+1}\mathbf{w}^f_{k+1}) \tag{3.7}$$

Analysis error covariance:

$$\mathbf{P}^a_{k+1} = (\mathbf{I} - \tilde{\mathbf{K}}_{k+1}\tilde{\mathbf{H}}_{k+1})\mathbf{P}^f_{k+1}(\mathbf{I} - \tilde{\mathbf{K}}_{k+1}\tilde{\mathbf{H}}_{k+1})^T + \tilde{\mathbf{K}}_{k+1}\mathbf{R}\tilde{\mathbf{K}}^T_{k+1}. \tag{3.8}$$

If the Kalman gain $\tilde{\mathbf{K}}$ has been computed exactly this reduces to

$$\mathbf{P}^a_{k+1} = (\mathbf{I} - \tilde{\mathbf{K}}_{k+1}\tilde{\mathbf{H}}_{k+1})\mathbf{P}^f_{k+1}. \tag{3.9}$$

We note that the optimality of the Kalman filter solution depends on the assumptions underlying the equations being accurate. If they do not hold then this quality will be lost.

3.3 The Extended Kalman Filter

The Kalman filter theory can be generalised for the case where the system model and/ or observation operator are non-linear by linearising around a background state. This gives the extended Kalman filter (EKF) (Gelb (1974), Jazwinski (1970)). The steps of the EKF algorithm are the same as for the standard Kalman filter except that the state forecast (3.4) is made using the full non-linear model and the matrices $\mathbf{F}$ and $\tilde{\mathbf{H}}_k$ in equations (3.5) to (3.9) are replaced by the tangent linear model of the non-linear model forecast operator $\tilde{\mathbf{f}}$ and (in the case of indirect observations) the tangent linear of the non-linear observation operator $\tilde{\mathbf{h}}_k$.

To summarise, we have

State forecast:

$$\mathbf{w}^f_{k+1} = \tilde{\mathbf{f}}(\mathbf{w}^a_k) \tag{3.10}$$

Error covariance forecast:

$$\mathbf{P}^f_{k+1} = \mathbf{F}_k\mathbf{P}^a_k\mathbf{F}^T_k, \tag{3.11}$$

where

$$\mathbf{F}_k = \left.\frac{\partial\tilde{\mathbf{f}}}{\partial\mathbf{w}}\right|_{\mathbf{w}^a_k} = \left.\begin{pmatrix} \frac{\partial\mathbf{f}(\mathbf{z},\mathbf{p})}{\partial\mathbf{z}} & \frac{\partial\mathbf{f}(\mathbf{z},\mathbf{p})}{\partial\mathbf{p}} \\ \mathbf{0} & \mathbf{I} \end{pmatrix}\right|_{\mathbf{z}^a_k,\mathbf{p}^a_k} \tag{3.12}$$

is the Jacobian of the augmented system forecast model evaluated at the current analysis state $\mathbf{w}^a_k$ (see appendix A).

Although the approximations made by the EKF make the optimisation problem easier to solve they do so at the expense of the optimality of the solution. The optimal analysis property of the standard linear Kalman filter no longer holds and the actual analysis error may differ considerably from that implied by equation (3.8).

The Kalman filter and EKF methods are compuationally much costlier than 3D Var; the updating of the error covariance matrices requires the equivalent of $O(m)$ model integrations, where m is dimension of the model state, plus adjoint and tangent linear models must be developed. If m is large the scheme becomes prohibitively expensive. Implementation of the full Kalman filter equations is therefore impracticable for systems of high dimension and in practice $\mathbf{P^f}$ is kept constant or a much simpler updating is performed. However, the equations provide a useful starting point for the design and development of approximate algorithms, examples of which include the Ensemble Kalman filter (EnKF) (Evensen (1994), Houtekamer and Mitchell (2005)) and the reduced rank Kalman filter (Fisher (1998)).

4 State augmentation and parameter estimation

Although the technique of state augmentation is straightforward in theory, practical implementation of the approach relies strongly on the relationships between the parameters and state components being well defined and assumes that we have sufficient knowledge to reliably describe them. Since it is not possible to observe the parameters directly, the parameter updates are only influenced by the observations through the cross covariances that describe the correlations between the error of the model state estimate and the error of the model parameter estimate (Martin (2000), Smith et al. (2009)).

In basic state estimation the background error covariances govern how information is spread throughout the model domain, passing information from observed to unobserved regions and smoothing data if there is a mismatch between the resolution of the model and the density of the observations. For the augmented system, it is the state-parameter cross covariances, given by the off diagonal blocks of the augmented background error covariance matrix $\tilde{\mathbf{B}}$, that pass information from the observed variables to update/ improve the estimates of the unobserved parameters. This is a crucial point; if the state-parameter cross covariances are inappropriately modelled the quality of the parameter estimates will be affected. Since the correct error statistics of the system are generally unknown we have to approximate them in some manner. Constructing a realistic representation of the background error covariances is one of the key challenges of data assimilation.

Initial work with a simple 1D linear model (Smith et al. (2008), Smith et al. (2009)) indicated that whilst the assumption of static covariances made by the 3D Var algorithm is sufficient for state estimation it is insufficient for parameter estimation as it does not provide an adequate representation of the state-parameter cross covariances required by the augmented system. In order to update the parameters these covariances need to be flow dependent. However, as already noted, using methods such as the Kalman filter equations to explicitly propagate the covariances is computationally expensive and requires adjoint and tangent linear models. Here we propose a hybrid approach by combining the 3D Var and EKF techniques. A simplified version of the extended Kalman filter forecast step is used to estimate the state-parameter forecast error cross covariances and this is then combined with an empirical, static approximation of the state background error covariances. We give details of the formulation of this new approach in the next section.

5 Background (forecast) error covariances

We can partition the forecast error covariance matrix (3.11) as follows

$$\mathbf{P}_k^f = \begin{pmatrix} \mathbf{P}^f_{\mathbf{z}\mathbf{z}_k} & \mathbf{P}^f_{\mathbf{z}\mathbf{p}_k} \\ (\mathbf{P}^f_{\mathbf{z}\mathbf{p}_k})^T & \mathbf{P}^f_{\mathbf{p}\mathbf{p}_k} \end{pmatrix}. \tag{5.1}$$

Here $\mathbf{P}^f_{\mathbf{z}\mathbf{z}_k} \in \mathbb{R}^{m\times m}$ is the forecast error covariance matrix for the state vector $\mathbf{z}_k$ at time t_k, $\mathbf{P}^f_{\mathbf{p}\mathbf{p}_k} \in \mathbb{R}^{q\times q}$ is the covariance matrix of the errors in the parameter vector $\mathbf{p}_k$ and $\mathbf{P}^f_{\mathbf{z}\mathbf{p}_k} \in \mathbb{R}^{m\times q}$ is the covariance matrix for the cross correlations between the forecast errors in the state and parameter vectors.

5.1 State background (forecast) error covariance

The standard approach in 3D Var is to assume that the background error covariances are homogeneous and isotropic. The state background error covariance matrix, which we will denote $\mathbf{B}_{\mathbf{z}\mathbf{z}}$, is then equal to the

product of the estimated error variance and a correlation matrix defined using a pre-specified correlation function. Here we use the correlation function (Rodgers (2000))

$$b_{ij} = \sigma_b^2 \rho^{|i-j|}, \qquad i, j = 1, \ldots, m, \tag{5.2}$$

where element b_{ij} defines the covariance between components i and j of the state background error vector $\boldsymbol{\varepsilon}_z = \mathbf{z}^b - \mathbf{z}^t$. Here $\rho = \exp(-\Delta x/L)$ where Δx is the model grid spacing and L is a correlation length scale that is adjusted empirically, and σ_b^2 is the state background error variance. The reason for choosing this covariance matrix is that its inverse can be calculated explicitly and has a particularly simple tridiagonal form (Smith et al. (2008)).

5.2 State-parameter cross covariance

Taking the EKF equations as a guide and considering the form of the error covariance forecast for a single step of the filter we construct a simplified method for propagating the state-parameter cross covariances.

To simplify, we assume that the observations are linearly related to the model state and taken at fixed locations, so that

$$\tilde{\mathbf{H}}_k = \tilde{\mathbf{H}} \equiv (\mathbf{H}\ \mathbf{0}) \tag{5.3}$$

for all k, where $\mathbf{H} \in \mathbb{R}^{r \times m}$.

Similarly for the observation error covariance matrix we set

$$\mathbf{R}_k = \mathbf{R}. \tag{5.4}$$

where $\mathbf{R}$ is a constant diagonal matrix.

The Kalman gain (3.6) can now be written as

$$\begin{aligned} \tilde{\mathbf{K}}_k &= \begin{pmatrix} \mathbf{P}^f_{\mathbf{z}\mathbf{z}_k} \\ (\mathbf{P}^f_{\mathbf{z}\mathbf{p}_k})^T \end{pmatrix} \mathbf{H}^T (\mathbf{H}\mathbf{P}^f_{\mathbf{z}\mathbf{z}_k}\mathbf{H}^T + \mathbf{R})^{-1} \\ &\stackrel{\text{def}}{=} \begin{pmatrix} \mathbf{K}_{\mathbf{z}_k} \\ \mathbf{K}_{\mathbf{p}_k} \end{pmatrix}, \end{aligned} \tag{5.5}$$

where $\mathbf{K}_{\mathbf{z}_k} \in \mathbb{R}^{m \times r}$ and $\mathbf{K}_{\mathbf{p}_k} \in \mathbb{R}^{q \times r}$.

Suppose we start at time t_k with analysis error covariance matrix

$$\mathbf{P}^a_k = \begin{pmatrix} \mathbf{P}^a_{\mathbf{z}\mathbf{z}_k} & \mathbf{P}^a_{\mathbf{z}\mathbf{p}_k} \\ (\mathbf{P}^a_{\mathbf{z}\mathbf{p}_k})^T & \mathbf{P}^a_{\mathbf{p}\mathbf{p}_k} \end{pmatrix} \in \mathbb{R}^{(m+q)\times(m+q)}, \tag{5.6}$$

where $\mathbf{P}^a_{\mathbf{z}\mathbf{z}} \in \mathbb{R}^{m \times m}$, $\mathbf{P}^a_{\mathbf{z}\mathbf{p}} \in \mathbb{R}^{m \times q}$ and $\mathbf{P}^a_{\mathbf{p}\mathbf{p}} \in \mathbb{R}^{q \times q}$.

If we denote

$$\mathbf{M}_k = \left.\frac{\partial \mathbf{f}(\mathbf{z}, \mathbf{p})}{\partial \mathbf{z}}\right|_{\mathbf{z}^a_k, \mathbf{p}^a_k} \qquad \text{and} \qquad \mathbf{N}_k = \left.\frac{\partial \mathbf{f}(\mathbf{z}, \mathbf{p})}{\partial \mathbf{p}}\right|_{\mathbf{z}^a_k, \mathbf{p}^a_k}, \tag{5.7}$$

where $\mathbf{M}_k \in \mathbb{R}^{m \times m}$ and $\mathbf{N}_k \in \mathbb{R}^{m \times q}$, we can re-write (3.12) as

$$\mathbf{F}_k = \begin{pmatrix} \mathbf{M}_k & \mathbf{N}_k \\ \mathbf{0} & \mathbf{I} \end{pmatrix}. \tag{5.8}$$

The error covariance forecast (3.11) is then given by

$$\begin{aligned}
\mathbf{P}^f_{k+1} &= \begin{pmatrix} \mathbf{M}_k & \mathbf{N}_k \\ \mathbf{0} & \mathbf{I} \end{pmatrix} \begin{pmatrix} \mathbf{P}^a_{\mathbf{zz}_k} & \mathbf{P}^a_{\mathbf{zp}_k} \\ (\mathbf{P}^a_{\mathbf{zp}_k})^T & \mathbf{P}^a_{\mathbf{pp}_k} \end{pmatrix} \begin{pmatrix} \mathbf{M}_k^T & \mathbf{0} \\ \mathbf{N}_k^T & \mathbf{I} \end{pmatrix} \\
&= \begin{pmatrix} \mathbf{M}_k\mathbf{P}^a_{\mathbf{zz}_k} + \mathbf{N}_k(\mathbf{P}^a_{\mathbf{zp}_k})^T & \mathbf{M}_k\mathbf{P}^a_{\mathbf{zp}_k} + \mathbf{N}_k\mathbf{P}^a_{\mathbf{pp}_k} \\ (\mathbf{P}^a_{\mathbf{zp}_k})^T & \mathbf{P}^a_{\mathbf{pp}_k} \end{pmatrix} \begin{pmatrix} \mathbf{M}_k^T & \mathbf{0} \\ \mathbf{N}_k^T & \mathbf{I} \end{pmatrix} \\
&= \begin{pmatrix} \mathbf{M}_k\mathbf{P}^a_{\mathbf{zz}_k}\mathbf{M}_k^T + \mathbf{N}_k(\mathbf{P}^a_{\mathbf{zp}_k})^T\mathbf{M}_k^T + \mathbf{M}_k\mathbf{P}^a_{\mathbf{zp}_k}\mathbf{N}_k^T + \mathbf{N}_k\mathbf{P}^a_{\mathbf{pp}_k}\mathbf{N}_k^T & \mathbf{M}_k\mathbf{P}^a_{\mathbf{zp}_k} + \mathbf{N}_k\mathbf{P}^a_{\mathbf{pp}_k} \\ (\mathbf{P}^a_{\mathbf{zp}_k})^T\mathbf{M}_k^T + \mathbf{P}^a_{\mathbf{pp}_k}\mathbf{N}_k^T & \mathbf{P}^a_{\mathbf{pp}_k} \end{pmatrix}
\end{aligned} \tag{5.9}$$

We do not want to recalculate (5.9) at every time step so we make some simplifying assumptions. We substitute the state forecast error covariance matrix $\mathbf{P}^f_{\mathbf{zz}_k}$ with our fixed approximation (5.2),

$$\mathbf{P}^f_{\mathbf{zz}_k} = \mathbf{B}_{\mathbf{zz}} \qquad \text{for all } k. \tag{5.10}$$

We assume that the parameter error covariance matrix is also fixed

$$\mathbf{P}^f_{\mathbf{pp}_k} = \mathbf{B}_{\mathbf{pp}} \qquad \text{for all } k, \tag{5.11}$$

and we assume that the state-parameter cross covariances are initially zero. This leads us to propose the following approximation for the augmented forecast error covariance matrix

$$\tilde{\mathbf{B}}_{k+1} = \begin{pmatrix} \mathbf{B}_{\mathbf{zz}} & \mathbf{N}_k\mathbf{B}_{\mathbf{pp}} \\ \mathbf{B}_{\mathbf{pp}}\mathbf{N}_k^T & \mathbf{B}_{\mathbf{pp}} \end{pmatrix}. \tag{5.12}$$

In other words, all elements of the background error covariance matrix (5.12) are kept fixed except the cross covariance terms

$$\mathbf{B}_{\mathbf{zp}_k} = \mathbf{N}_k\mathbf{B}_{\mathbf{pp}}, \tag{5.13}$$

which are updated at each new analysis time by recalculating the matrix $\mathbf{N}_k$, where $\mathbf{N}_k$ is the Jacobian of the forecast model with respect to the parameters, as defined in equation (5.7). Explicitly calculating the Jacobian of complex functions can be a difficult task, requiring complicated derivatives if done analytically or being computationally costly if done numerically. We continue in our pursuit of a simplistic approach and use finite differences to approximate $\mathbf{N}_k$. Further details of this calculation are given in section 6.2 for our specific model.

The analysis $\mathbf{w}^a_k$ is found by substituting the matrix (5.12) into the 3D Var cost function (3.1) and minimising. When the observation operator $\mathbf{h}$ is linear the minimum of (5.12) can be written explicitly as

$$\mathbf{w}^a_k = \mathbf{w}^b_k + \tilde{\mathbf{K}}_k(\mathbf{y}_k - \tilde{\mathbf{H}}\mathbf{w}^b_k), \tag{5.14}$$

where

$$\begin{aligned}
\tilde{\mathbf{K}}_k &= \tilde{\mathbf{B}}_k\tilde{\mathbf{H}}^T(\tilde{\mathbf{H}}\tilde{\mathbf{B}}_k\tilde{\mathbf{H}}^T + \mathbf{R})^{-1} \\
&\stackrel{\text{def}}{=} \begin{pmatrix} \mathbf{K}_{\mathbf{z}_k} \\ \mathbf{K}_{\mathbf{p}_k} \end{pmatrix}.
\end{aligned} \tag{5.15}$$

Although in practice the cost function (3.1) is minimised numerically, the analytical form for the solution (5.14) is useful for helping to understand the role of the state-parameter cross-covariances.

Separating (5.14) into state and parameter parts gives

$$\mathbf{z}^a_k = \mathbf{z}^b_k + \mathbf{K}_{\mathbf{z}_k}(\mathbf{y}_k - \mathbf{H}\mathbf{z}^b_k) \tag{5.16}$$

$$\mathbf{p}^a_k = \mathbf{p}^b_k + \mathbf{K}_{\mathbf{p}_k}(\mathbf{y}_k - \mathbf{H}\mathbf{z}^b_k) \tag{5.17}$$

The gain matrices (5.15) are given by

$$\mathbf{K}_{\mathbf{z}_k} = \mathbf{B}_{\mathbf{zz}}\mathbf{H}^T(\mathbf{H}\mathbf{B}_{\mathbf{zz}}\mathbf{H}^T + \mathbf{R})^{-1} \quad (5.18)$$

$$\mathbf{K}_{\mathbf{p}_k} = \mathbf{B}_{\mathbf{pp}}\mathbf{N}_k^T\mathbf{H}^T(\mathbf{H}\mathbf{B}_{\mathbf{zz}}\mathbf{H}^T + \mathbf{R})^{-1} \quad (5.19)$$

Note that since we are assuming that $\mathbf{B_{zz}}$ and $\mathbf{H}$ are constant matrices, the state gain $\mathbf{K}_{\mathbf{z}_k} = \mathbf{K_z}$ is fixed for all time. The analysis equation for the state vector (5.16) is therefore the same as would be derived if the 3D Var method was being used for state estimation only.

The innovation vector $(\mathbf{y}_k - \mathbf{H}\mathbf{z}_k^b)$ is exactly the same in equations (5.16) and (5.17), as is the expression inside the inverse for the state and parameter gain matrices (5.18) and (5.19). Both the state and parameters are updated according to the discrepancies between the observations and the model predicted state, the difference lies in exactly how this information is used. This is determined by our choice of $\mathbf{B_{zz}}$ and $\mathbf{B_{zp}}$. We have already stated that, in order to reliably estimate the model parameters, the matrix $\mathbf{B_{zp}}$ must adequately describe the relationship between the errors in the state estimate and the errors in the parameters. Our proposed approximation to $\mathbf{B_{zp}}$ (5.13) does this by combining the relationship between the parameters (described by $\mathbf{B_{pp}}$) with the way changes in the parameters effect the forecast model (described by $\mathbf{N}_k$).

6 The model

We investigate the application of our hybrid scheme to the problem of morphodynamic model parameter estimation using a simple 1D non-linear model of bed-form propagation. This model has two uncertain parameters that need to be set and is based on the 1D sediment conservation equation (Soulsby (1997)).

6.1 The sediment conservation equation

The sediment conservation equation can be used to describe changes in bathymetry due to flow induced sediment transport. In one dimension it is written as

$$\frac{\partial z}{\partial t} = -\left(\frac{1}{1-\varepsilon}\right)\frac{\partial q}{\partial x}, \quad (6.1)$$

in the x direction, where $z(x,t)$ is the bathymetry, t is the time, q is the total (suspended and bedload) sediment transport rate, and ε is the sediment porosity. If $\frac{\partial z}{\partial t}$ is positive accretion is occurring, and if $\frac{\partial z}{\partial t}$ is negative erosion is occurring.

The sediment transport rate q is calculated using a power law equation (Grass (1981))

$$q = Au^n \quad (6.2)$$

where $u = u(x,t)$ is the current in the x direction and A and n are parameters whose values need to be set. The parameter A is a dimensional constant whose value depends on various properties of the sediment and water, such as flow depth and velocity range, sediment grain size and kinematic viscosity. van Rijn (1993) gives a formula that can be used to obtain an approximation to A for a given set of sediment and water properties. The derivation of the parameter n is less clear. It is usually set by fitting to field data and generally takes a value in the range $1 \leq n \leq 4$.

The power law expression (6.2) is one of the most basic sediment transport flux formulae and is a very simplified version of a complex set of formulae derived by van Rijn (1993). Numerous alternative formulae have been proposed, many of which are presented in Soulsby (1997). These are typically based on a mixture of fundamental physics and empirical results and the choice of which to use generally depends on the particular situation being modelled. In Pinto et al. (2006) the strengths, weaknesses and applicability of five popular formulae are assessed, references to other comparision studies are also given.

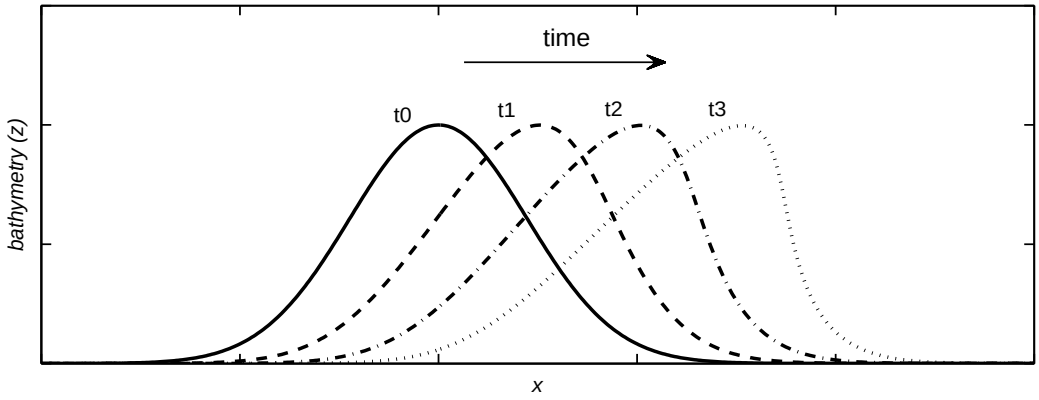

Figure 6.1: Solutions to the non-linear advection equation for Gaussian initial

To solve (6.1) we re-write it in the quasi-linear form

$$\frac{\partial z}{\partial t} + a(z,q)\frac{\partial z}{\partial x} = 0, \tag{6.3}$$

where

$$a(z,q) = \left(\frac{1}{1-\varepsilon}\right)\frac{\partial q}{\partial z}. \tag{6.4}$$

The coefficient $a(z,q)$ is the advection velocity or bed celerity. It is a non-linear function, depending on the bathymetry z both directly and through the sediment transport rate q.

To close the problem, we assume that the water height h and flux F are constant in space and set

$$F = u(h-z). \tag{6.5}$$

Using (6.5) we can re-write (6.2) as

$$q = A\left(\frac{F}{h-z}\right)^n. \tag{6.6}$$

Substituting (6.6) into (6.4) gives

$$a(z) = \left(\frac{nAF^n}{1-\varepsilon}\right)(h-z)^{-(n+1)}. \tag{6.7}$$

The bed celerity is now a function of the bed height z only. We assume that the water height h, flux F and sediment porosity ε are known constant values but that the values of the parameters A and n are uncertain.

As discussed in Smith et al. (2007) we can use the method of characteristics to derive an analytic solution to the advection form of the sediment conservation equation (6.3). Figure 6.1 illustrates the evolution of the solution for a smooth, initially symmetric, isolated bed-form generated using Gaussian initial data. As time increases the bed propagates across the model domain with velocity (6.7). Since $a(z)$ is non-linear the bed profile becomes distorted and eventually overturns. Whilst this type of solution would make sense in some contexts (such as a breaking wave) we wouldn't expect it here. In real life, this overturning is prevented by natural phenomena such as bed-slope effects (Soulsby (1997)). We create a more physically realistic solution that remains smooth and single valued by adding a small diffusive term to the right hand side of (6.3). Our model then becomes an advection-diffusion equation. We calculate the solution numerically using a combined semi-Lagrangian Crank-Nicolson scheme based on that presented in Spiegelman and Katz (2006).

Since we are assuming that the parameters are constant, the evolution equations for A and n are taken as

$$\frac{dA}{dt} = 0 \quad \text{and} \quad \frac{dn}{dt} = 0. \tag{6.8}$$

Equations (6.8) together with the bed updating equation (6.3) constitute our augmented system model (2.4).

We use this simple system to test our hybrid approach to modelling the background error covariances. We investigate whether, given an uncertain initial bathymetry and approximated values of A and n, and using synthetic observations taken from the true solution, our proposed method can successfully deliver both an accurate estimate of the current bathymetry and accurate estimates of the uncertain parameters thereby improving the predictive ability of our model.

6.2 State-parameter cross covariances for the simple non-linear model

Before we can implement our augmented scheme we need to construct the state-parameter cross covariance matrix $\mathbf{B_{zp}}$ as outlined in section 5.2.

We include the uncertain model parameters A and n in the parameter vector $\mathbf{p}_k \in \mathbb{R}^2$

$$\mathbf{p}_k = \begin{pmatrix} A_k \\ n_k \end{pmatrix}, \tag{6.9}$$

where A_k and n_k are the model estimated values of parameters A and n at time t_k.

This is added to a vector $\mathbf{z}_k \in \mathbb{R}^m$ representing the bathymetry at discrete points to give the augmented state vector (2.5).

Our approximation of the state-parameter cross covariances (5.13) requires an approximation of the matrix $\mathbf{N}_k$, the Jacobian of the forecast model with respect to $\mathbf{p}_k$. For our two parameter model this is defined as

$$\mathbf{N}_k = \begin{pmatrix} \frac{\partial \mathbf{f}(\mathbf{z},\mathbf{p})}{\partial A_k} & \frac{\partial \mathbf{f}(\mathbf{z},\mathbf{p})}{\partial n_k} \end{pmatrix}\Big|_{\mathbf{z}_k^a, \mathbf{p}_k^a}. \tag{6.10}$$

Writing the covariance matrix of the errors in the parameter vector $\mathbf{B_{pp}}$ as

$$\mathbf{B_{pp}} = \begin{pmatrix} \sigma_A^2 & \sigma_{An} \\ \sigma_{nA} & \sigma_n^2 \end{pmatrix}, \tag{6.11}$$

where $\sigma_A^2 = E(\varepsilon_A^2)$ and $\sigma_n^2 = E(\varepsilon_n^2)$ are the error variances for A and n respectively and $\sigma_{An} = \sigma_{nA} = E(\varepsilon_A \varepsilon_n)$ is the covariance between the errors in A and n. The state-parameter cross covariance matrix (5.13) is given by

$$\begin{aligned} \mathbf{B}_{\mathbf{zp}_k} &= \mathbf{N}_k \mathbf{B_{pp}} \\ &= \begin{pmatrix} \frac{\partial \mathbf{f}}{\partial A_k} & \frac{\partial \mathbf{f}}{\partial n_k} \end{pmatrix} \begin{pmatrix} \sigma_A^2 & \sigma_{An} \\ \sigma_{An} & \sigma_n^2 \end{pmatrix} \\ &= \begin{pmatrix} \sigma_A^2 \frac{\partial \mathbf{f}}{\partial A_k} + \sigma_{An} \frac{\partial \mathbf{f}}{\partial n_k} & \sigma_n^2 \frac{\partial \mathbf{f}}{\partial n_k} + \sigma_{An} \frac{\partial \mathbf{f}}{\partial A_k} \end{pmatrix} \end{aligned} \tag{6.12}$$

Rather than explicitly calculate the Jacobian matrix (6.10) at each new assimilation time t_k, we approximate using simple finite differences. Defining

$$\mathbf{z}_{k+1}^b = \mathbf{f}(\mathbf{z}_k^a, \mathbf{p}_k^a) \quad \text{and} \quad \hat{\mathbf{z}}_{k+1}^b = \mathbf{f}(\mathbf{z}_k^a, \hat{\mathbf{p}}_k^a) \tag{6.13}$$

we approximate $\frac{\partial \mathbf{f}}{\partial A}$ and $\frac{\partial \mathbf{f}}{\partial n}$ as follows,

$$\frac{\partial \mathbf{f}(\mathbf{z}_k^a, \mathbf{p}_k^a)}{\partial A} \approx \frac{\hat{\mathbf{z}}_{k+1}^b - \mathbf{z}_{k+1}^b}{\delta A} \tag{6.14}$$

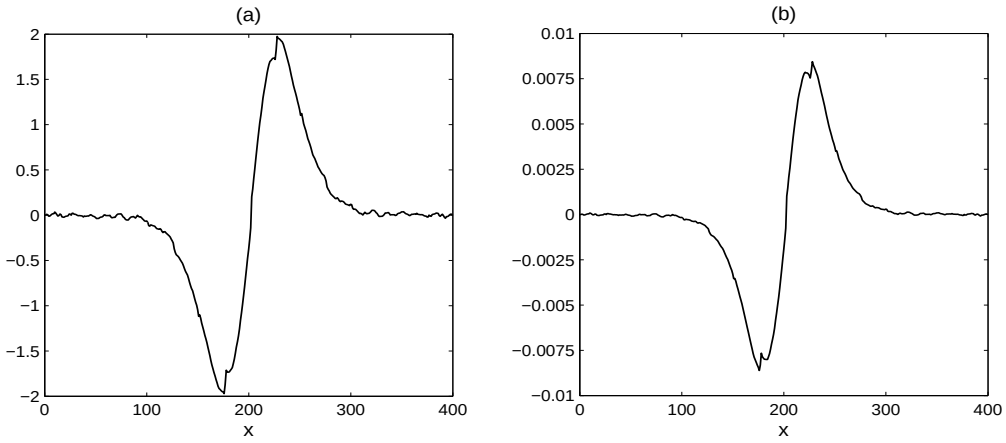

Figure 6.2: Approximating the matrix $\mathbf{N}_k$: (a) $\frac{\partial \mathbf{f}}{\partial A}$, and (b) $\frac{\partial \mathbf{f}}{\partial n}$ at $t = 0$ for an example assimilation run with $A_0 = 0.02ms^{-1}$, $\delta A = 10^{-5}$, $n_0 = 2.4$, $\delta n = 10^{-2}$.

where

$$\hat{\mathbf{p}}_k^a = \begin{pmatrix} A_k^a + \delta A \\ n_k^a \end{pmatrix}, \tag{6.15}$$

$\mathbf{p}_k^a$ is the current parameter estimate and δA is a small perturbation to the current approximation of the parameter A.

Similarly

$$\left.\frac{\partial \mathbf{f}}{\partial n}\right|_{\mathbf{z}_k^a, \mathbf{p}_k^a} \approx \frac{\hat{\mathbf{z}}_{k+1}^b - \mathbf{z}_{k+1}^b}{\delta n} \tag{6.16}$$

where

$$\hat{\mathbf{z}}_{k+1}^b = \mathbf{f}(\mathbf{z}_k^a, \hat{\mathbf{p}}_k^a) \quad \text{and} \quad \hat{\mathbf{p}}_k^a = \begin{pmatrix} A_k^a \\ n_k^a + \delta n \end{pmatrix},$$

and δn is a small perturbation to the current approximation of the parameter n.

Figures 6.2(a) and (b) show $\frac{\partial \mathbf{f}}{\partial A}$ and $\frac{\partial \mathbf{f}}{\partial n}$ calculated at for an example assimilation run. The model is run forward over a single time step; once using the current parameter estimate (a) A_k^a or (b) n_k^a and a second time using the perturbed value $A_k^a + \delta A$ (or $n_k^a + \delta n$). The difference between the two forecasts divided by the perturbation δA (or δn) is then calculated yielding the approximation (6.14) or (6.16) .

The effect on the model of a change in A or n is similar in both cases. As can be seen from equation (6.6) A and n affect the magnitude of the sediment transport rate and in turn the bed celerity (6.7). It is a feature of our choice of sediment transport flux formula (6.6) that the model is more sensitive to the parameter A than it is to n. Incorrect estimation of either parameter produces a phase error but the divergence of the model from the true solution is more rapid when the error is in A. If the current u in (6.2) is close or equal to $1\,\mathrm{ms}^{-1}$, a change in n will have little or no effect on the model.

A further problem is that of equifinality, that is, there exists a range of different parameter combinations that produce similar model behaviour (Navon (1997), Sorooshian and Gupta (1995)). This can lead to estimates that are, strictly speaking, 'incorrect' but that are in practice sufficiently accurate when used to forecast over short time periods. Our early work has found that if the state-parameter cross covariances are poorly specified, the tendency of the model is to compensate for errors in the value of n through A, i.e. an underestimated n value is offset by an overestimate of parameter A and vice versa. These issues will be discussed further in the following results section.

7 Results

We test our augmented scheme by running a series of identical twin experiments. We assume that our numerical model is perfect and generate a 'true' solution by running the model from a Gaussian initial

state with set parameter values $A = 0.002\,\mathrm{ms}^{-1}$ and $n = 3.4$. This solution is used to provide pseudo-observations for the data assimilation and also to evaluate the performance of our scheme. The model is then re-run with the data assimilation, starting from a perturbed initial bathymetry and with incorrect starting estimates of parameters A and n.

The assimilation process was carried out sequentially, with a new set of observations being assimilated every hour. The model was sampled on a regular grid with a spacing of $\Delta x = 1.0\,\mathrm{m}$ and the cost function was minimised iteratively using a quasi-Newton descent algorithm (Gill et al. (1981)). Observations were generated from the true solution at intervals of $25\Delta x$. Initially, they are assumed to be perfect and without any added noise (i.e. $\mathbf{y} = \mathbf{h}(\mathbf{z}^t)$); we therefore weight in their favour. In the examples shown the observation and state background error variances are set at a ratio of 1:5. The state background error covariance matrix $\mathbf{B_{zz}}$ is given by (5.2) and is kept fixed, as is the parameter background error covariance matrix $\mathbf{B_{pp}}$. The state-parameter cross covariance matrix $\mathbf{B_{zp}}$ is recalculated at each new assimilation time as described in section 6.2. At the end of each assimilation cycle the model parameters are updated and the state analysis is integrated forward using the model (with the new parameter values) to become the background state for the next analysis time.

7.1 Experiments

Figures 7.1 and 7.2 illustrate the impact incorrect parameter estimates can have on the modelled bathymetry by comparing model runs performed with and without data assimilation over a 24 hour period. In these examples, the parameter A is initially over estimated ($A_0 = 0.02\,\mathrm{ms}^{-1}$) and n under estimated ($n_0 = 2.4$). With no data assimilation (figure 7.1), the effect on the predictive ability of the model is marked/ considerable. The model bathymetry (dashed blue line) rapidly diverges away from the true bathymetry (solid red line). After 4 hours the model bathymetry has travelled further than the true bathymetry in 24 hours, and after 24 hours it has moved beyond the model domain.

Re-running the model with the augmented data assimilation scheme greatly improves the model predictions as is illustrated in figure 7.2. The dotted red line represents the true bathymetry, observations are given by circles, the background state by the dashed blue line and the analysis by the solid green line. At 24 hours it is almost impossible to distinguish between the predicted model bathymetry and the true bathymetry.

The corresponding parameter A and n updates are shown in figures 7.3 (a) and (b). Figures 7.4 (a) and (b) show the parameter updating for a second test case in which the situation is reversed so that A is underestimated ($A_0 = 0.0$) and n is overestimated ($n_0 = 4.4$). In both instances, the scheme retrieves the true A and n values to a high level of acccuracy. The convergence of the estimates is much slower in the second case. As we discussed in section 6.2, our model is much more sensitive to the choice of parameter A than it is to the parameter n. In this example, the low A estimate and means that the model predicted bathymetry does not diverge away from the true bathymety as quickly as when A is overestimated. Because the initial background bathymetry is relatively well defined/ prescribed, the time between successive assimilations is short and we are weighting towards the observations, the difference between the modelled and true bathymetry remains small. The observation minus background increments are therefore small, leading to small analysis increments and hence slower updating. In other words, the state estimation alone is good enough to compensate for the incorrect parameters over short timescales. We found that the convergence of the estimates could be improved by inflating the error variances (figure 7.5).

In these examples we have chosen A and n so that the initial errors $\varepsilon_A = A_0^b - A^t$ and $\varepsilon_n = n_0^b - n^t$ are of opposite sign. When A is over (under) estimated the increments in A need to be negative (positive), and the same applies for n. Both the state and parameters are updated according to the observations, exactly how the information in these observations is used depends on the background error covariance matrices. Specifically, the magnitude and direction of the parameter updates will depend on the state-parameter cross covariances $\mathbf{B}_{\mathbf{z}A}$ and $\mathbf{B}_{\mathbf{z}n}$ and these in turn depend on the error variances σ_A^2, σ_n^2 and cross covariance σ_{An}. To ensure that the parameters are updated correctly, our choice of σ_A^2, σ_n^2 and σ_{An} needs to be consistent with the true error statistics.

From section 6.2, figure 6.2, we see that $\frac{\partial \mathbf{f}}{\partial A}$ and $\frac{\partial \mathbf{f}}{\partial n}$ are always the same sign. Using definition (6.12), if the parameter cross covariance $\sigma_{An} \geq 0$ then the elements of $\mathbf{B}_{\mathbf{z}A}$ and $\mathbf{B}_{\mathbf{z}n}$ will also always have the same sign and so A and n will both be updated in the same direction. When the errors in A and n are in opposite directions we need $\mathbf{B}_{\mathbf{z}A}$ and $\mathbf{B}_{\mathbf{z}n}$ to take opposite signs. We can achieve this by setting $\sigma_{An} < 0$

and choosing a σ_A^2 and σ_n^2 that take account of the relative magnitude of the errors in the parameter estimates.

Figures 7.6 and 7.7 show the parameter estimates produced when the two test cases described above were repeated using $\sigma_{An} > 0$. The parameters A and n are now both updated in the same direction. The direction of the increments seems to be dominated by the direction of the error in the A estimate. This is most likely due to our model being more sensitive to small changes in A than n. The A estimates converge towards the true value of A but are less accurate than in the previous examples. In both cases, the scheme completely fails to find the correct n value.

Despite the inability to recover the correct n value, the model is still able to produce accurate predictions of the bathymetry as is illustrated in figure 7.8. The state analyses corresponding to the updates in figure 7.7 are not shown as they are almost identical to figure 7.8.

7.2 Imperfect observations

Figures 7.9 to 7.14 show the results of a further set of experiments investigating the effect of observational errors. This was done by adding random noise to the observations. The noise was defined to have a Gaussian distribution with mean of zero and standard deviation σ_o, where σ_o^2 is the observation error variance. Figures 7.9 and 7.11 show the estimates produced for initial parameter combinations $A_0 = 0.02\,\mathrm{ms}^{-1}$, $n_0 = 2.4$ and $A_0 = 0.0\,\mathrm{ms}^{-1}$, $n_0 = 4.4$ with $\sigma_o = 0.1$. This σ_o value is equivalent to 10% of maximum bed height and believed to represent a realistic level of measurement error. As we would expect, when the observations are noisy the resulting analysis and parameter estimates are also noisy. However, the oscillations in the A and n estimates appear to be approximately centered around their true values. If we calculate the time average of the current and preceeding estimates at each new assimilation time, as is shown in figures 7.10 and 7.12, we find that we are actually moving very close to the true A and n values.

In the above experiments, the background and observation error variances were set at a ratio of 5:1. In order for the maximum amount of information to be extracted from the observations, the weight given to the observations relative to the background must be correctly specified. The background error correlations play a key role in the filtering of the observational noise. When the observations are noisy, too much weight given to the observations relative to the background will produce a noisy analysis. We found that the size of the oscillations could be reduced by increasing the weight given to the background. Figures 7.15 and 7.16 show the parameter estimates obtained using $\sigma_o^2 = 0.01$, $\sigma_b^2 = 0.02$ and $\sigma_o^2 = 0.01$, $\sigma_b^2 = 0.01$ for the case $A_0 = 0.02\,\mathrm{ms}^{-1}$, $n_0 = 2.4$. The oscillations can be reduced even further by underweighting the observations, that is, using $\sigma_o = 0.1$ to generate the observation noise but inflating the value of σ_o^2 in the assimilation. This is illustrated in figures 7.17 and 7.18 for the combinations $\sigma_o^2 = 0.02$, $\sigma_b^2 = 0.01$ and $\sigma_o^2 = 0.05$, $\sigma_b^2 = 0.05$ respectively.

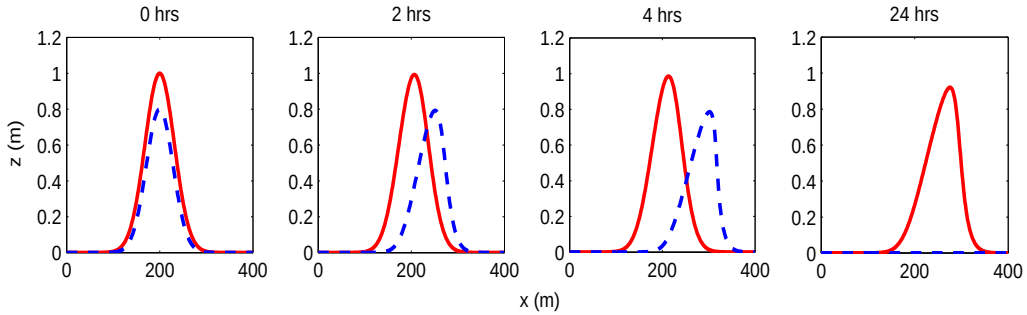

Figure 7.1: Model run with without data assimilation: the *solid red line* represents the true bathymetry $\mathbf{z}^t$ and the *dashed blue line* represents the predicted model bathymetry $\mathbf{z}^b$.

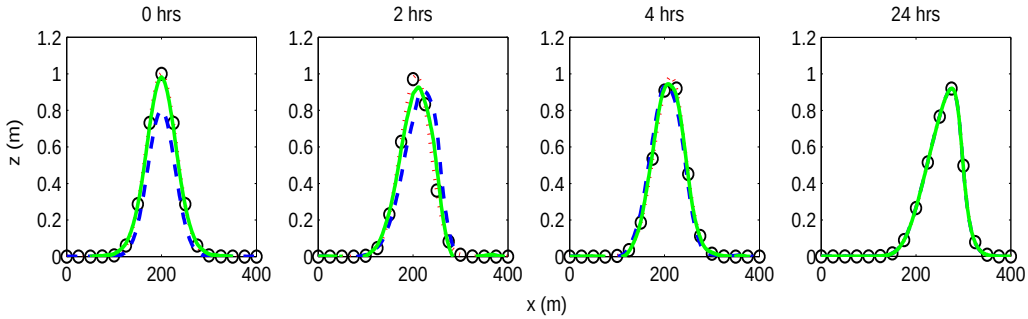

Figure 7.2: Model run with data assimilation: the *dotted red line* represents the true bathymetry $\mathbf{z}^t$, observations $\mathbf{y}$ are given by *circles*, the background $\mathbf{z}^b$ is given by the *dashed blue line* and the analysis $\mathbf{z}^a$ is given by the *solid green line*.

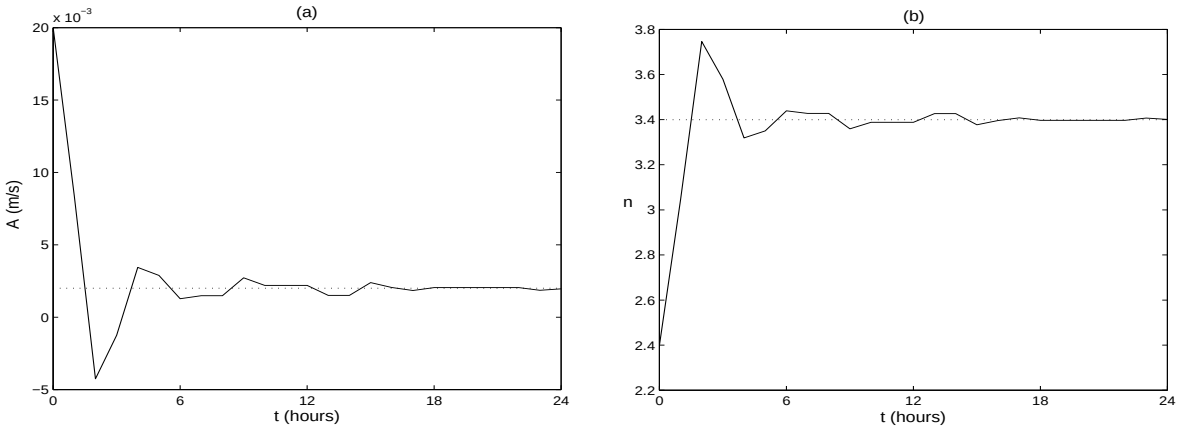

Figure 7.3: Parameter updates for initial estimates $A_0 = 0.02\text{ms}^{-1}$ and $n_0 = 2.4$.

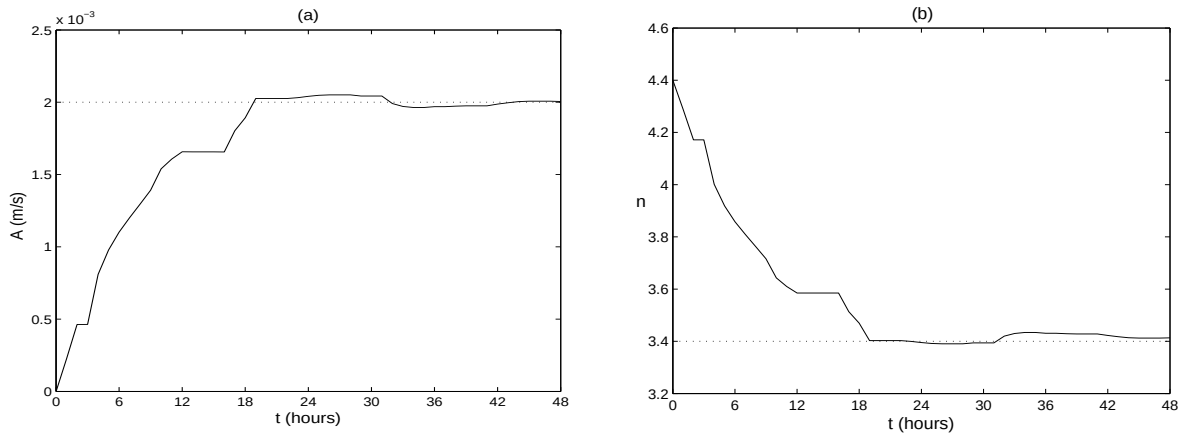

Figure 7.4: Parameter updates for initial estimates $A_0 = 0.0\,\mathrm{ms}^{-1}$ and $n_0 = 4.4$.

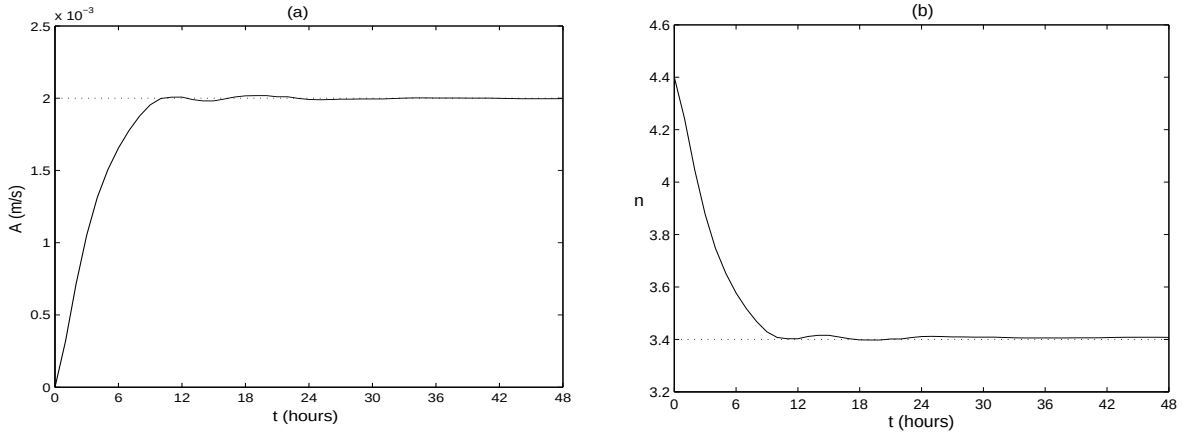

Figure 7.5: Parameter updates for initial estimates $A_0 = 0.0\,\mathrm{ms}^{-1}$ and $n_0 = 4.4$ using inflated error covariances.

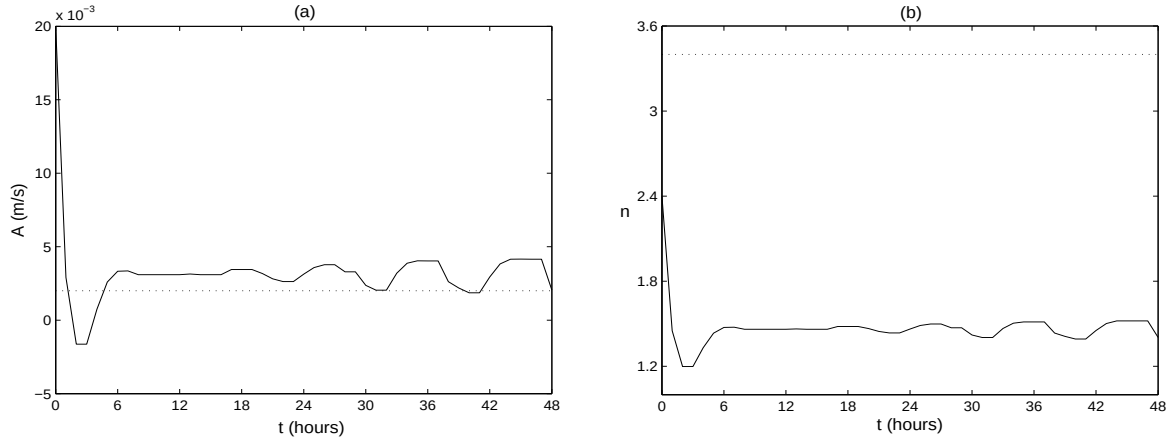

Figure 7.6: Incorrect parameter cross covariance: parameter updates for initial estimates $A_0 = 0.02\,\mathrm{ms}^{-1}$ and $n_0 = 2.4$.

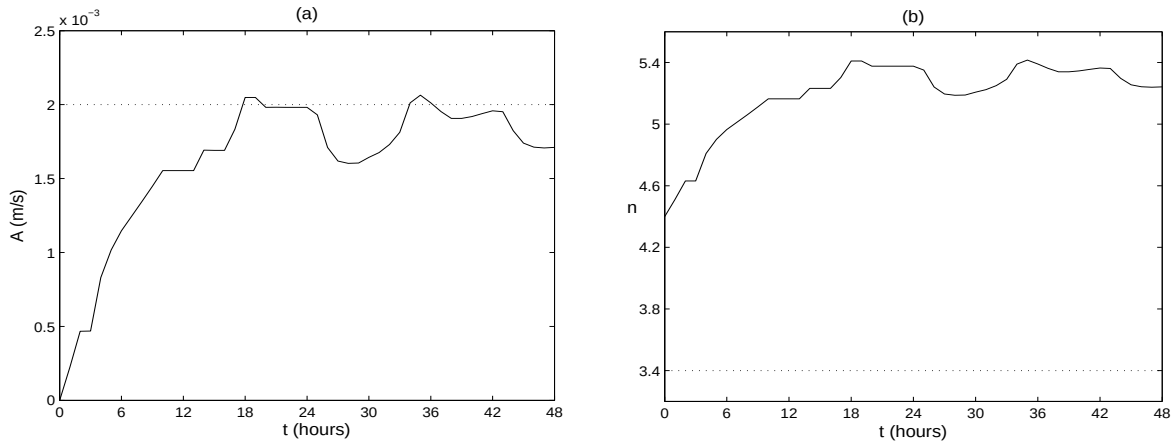

Figure 7.7: Incorrect parameter cross covariance: parameter updates for initial estimates $A_0 = 0.0\,\mathrm{ms}^{-1}$ and $n_0 = 4.4$.

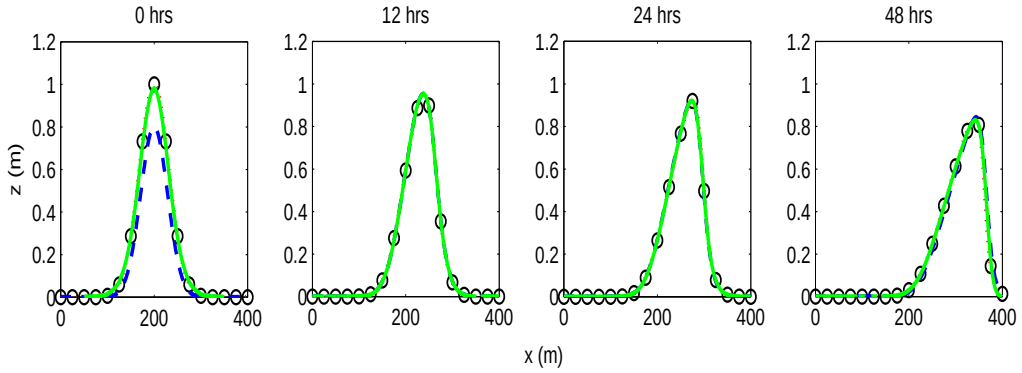

Figure 7.8: State analysis corresponding to parameter updates shown in figure 7.6: the *dotted red line* represents the true bathymetry $\mathbf{z}^t$, observations $\mathbf{y}$ are given by *circles*, the background $\mathbf{z}^b$ is given by the *dashed blue line* and the analysis $\mathbf{z}^a$ is given by the *solid green line*.

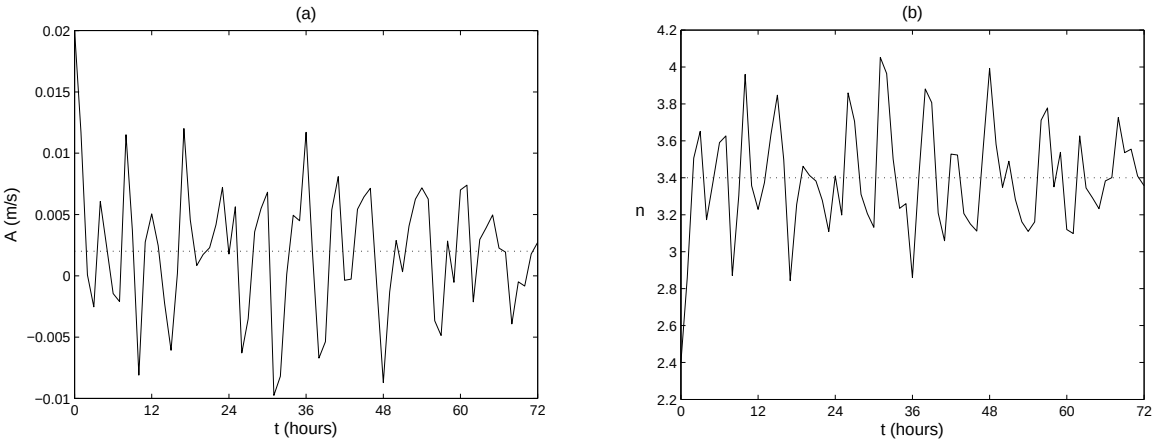

Figure 7.9: Adding noise to observations: parameter updates for initial estimates $A_0 = 0.02\,\mathrm{ms}^{-1}$ and $n_0 = 2.4$, $\sigma_o = 0.1$.

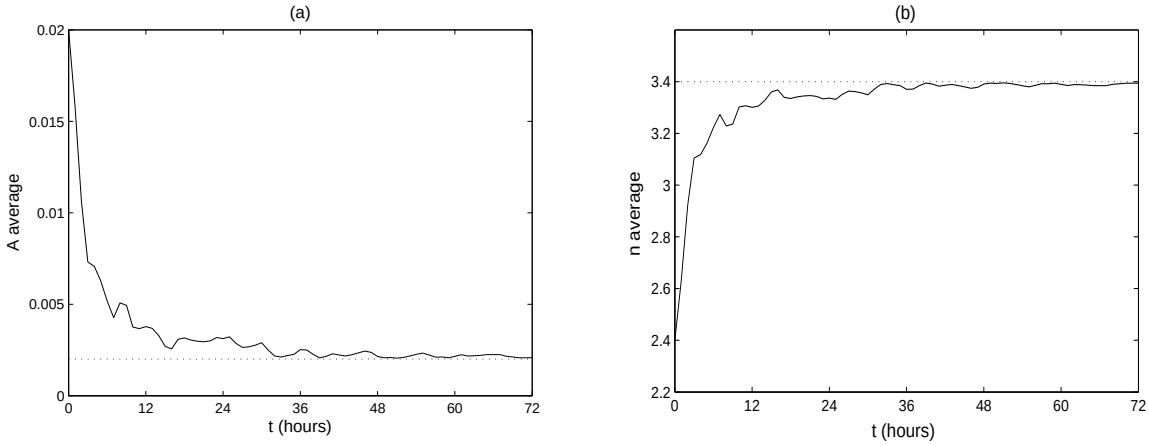

Figure 7.10: Adding noise to observations: averaged parameter updates for initial estimates $A_0 = 0.02\,\mathrm{ms}^{-1}$ and $n_0 = 2.4$, $\sigma_o = 0.1$.

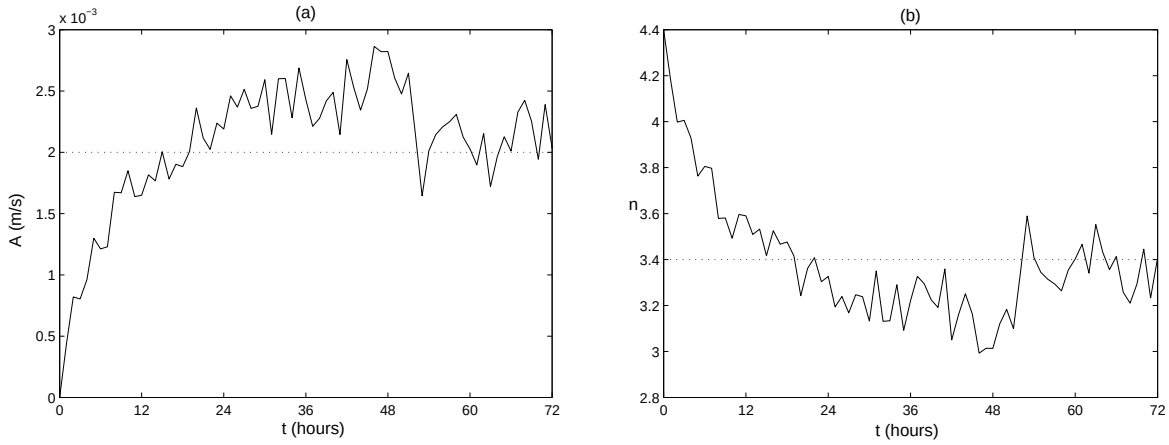

Figure 7.11: Adding noise to observations: parameter updates for initial estimates $A_0 = 0.0\,\mathrm{ms}^{-1}$ and $n_0 = 4.4$, $\sigma_o = 0.1$.

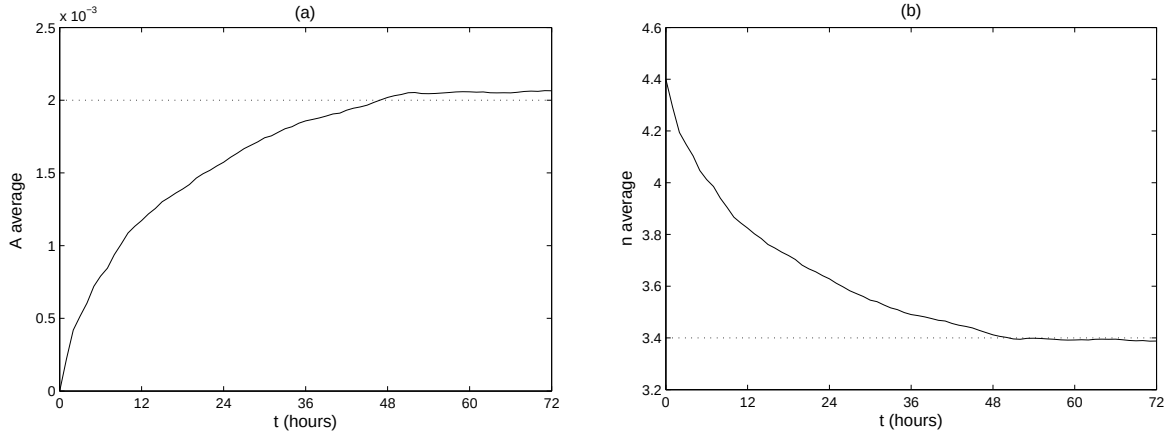

Figure 7.12: Adding noise to observations: averaged parameter updates for initial estimates $A_0 = 0.0\mathrm{ms}^{-1}$ and $n_0 = 4.4$, $\sigma_o = 0.1$.

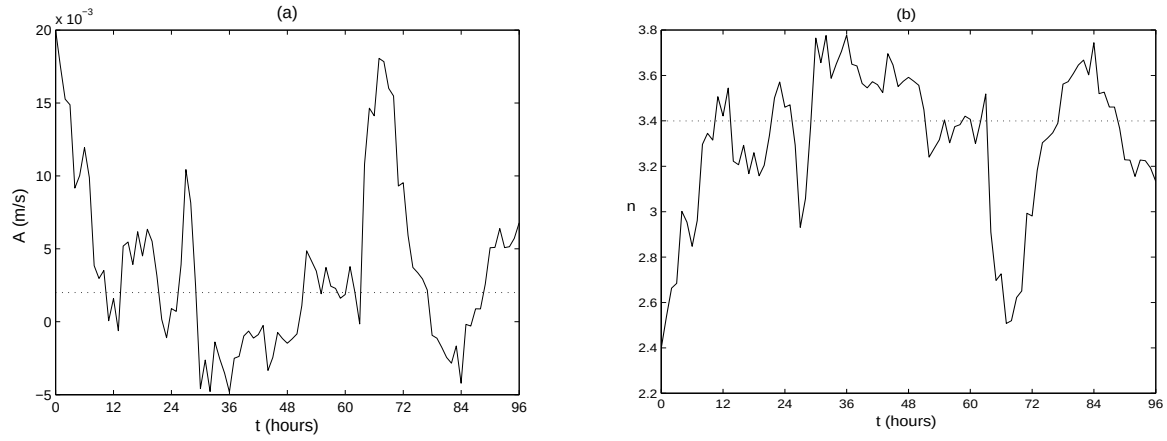

Figure 7.13: Adding noise to observations: parameter updates for initial estimates $A_0 = 0.02\,\mathrm{ms}^{-1}$ and $n_0 = 2.4$, $\sigma_o = 0.2$.

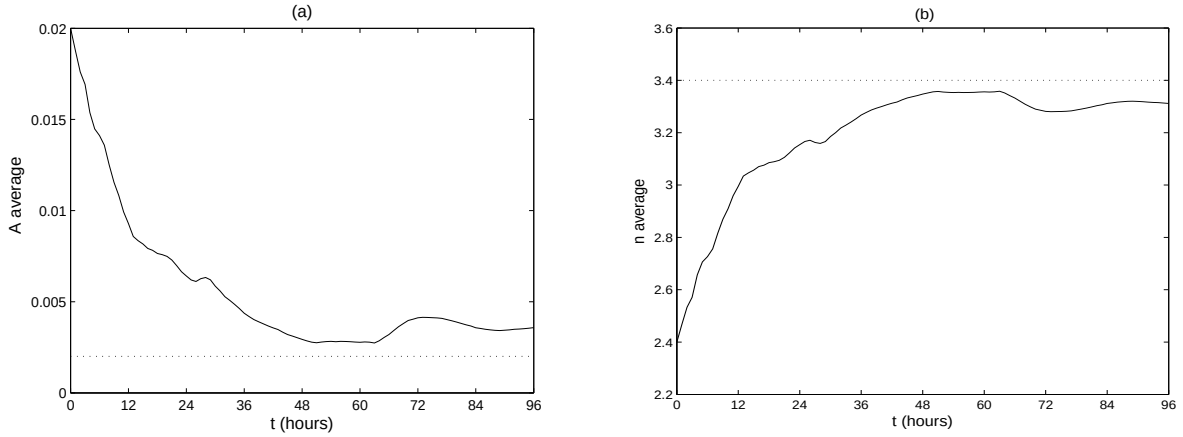

Figure 7.14: Adding noise to observations: averaged parameter updates for initial estimates $A_0 = 0.02\,\mathrm{ms}^{-1}$ and $n_0 = 2.4$, $\sigma_o = 0.2$.

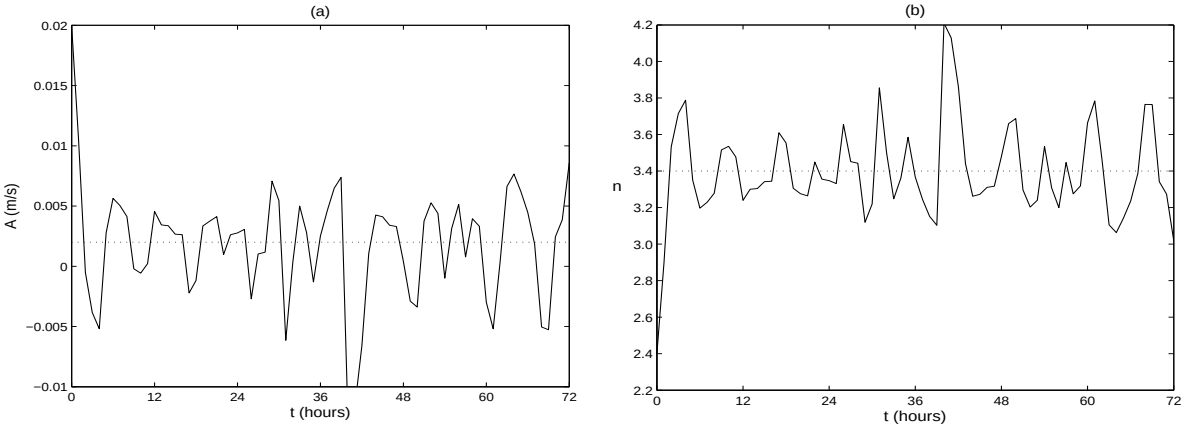

Figure 7.15: Increasing weight given to the background state: $\sigma_o^2 = 0.01$, $\sigma_b^2 = 0.02$, parameter updates for initial estimates $A_0 = 0.02\,\mathrm{ms}^{-1}$ and $n_0 = 2.4$.

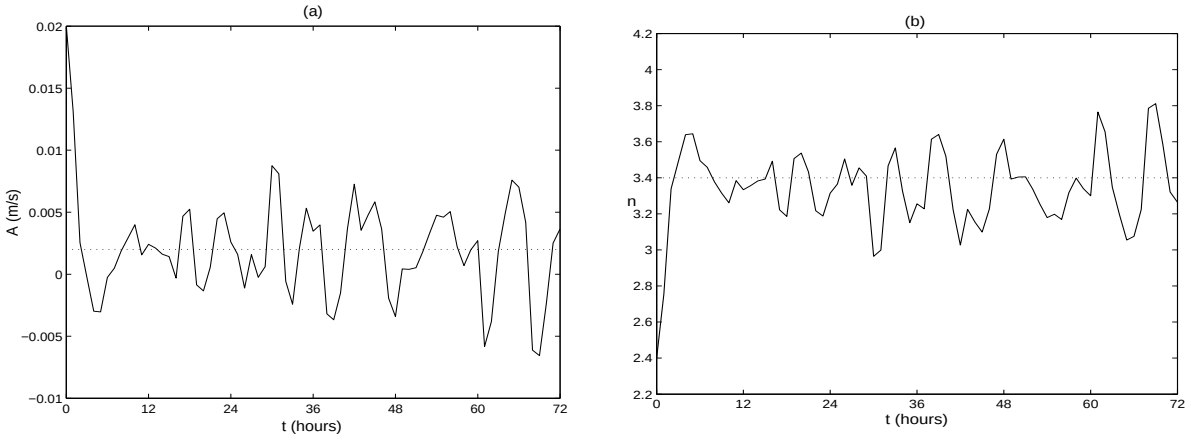

Figure 7.16: Increasing weight given to the background state: $\sigma_o^2 = 0.01$, $\sigma_b^2 = 0.01$, parameter updates for initial estimates $A_0 = 0.02\,\mathrm{ms}^{-1}$ and $n_0 = 2.4$.

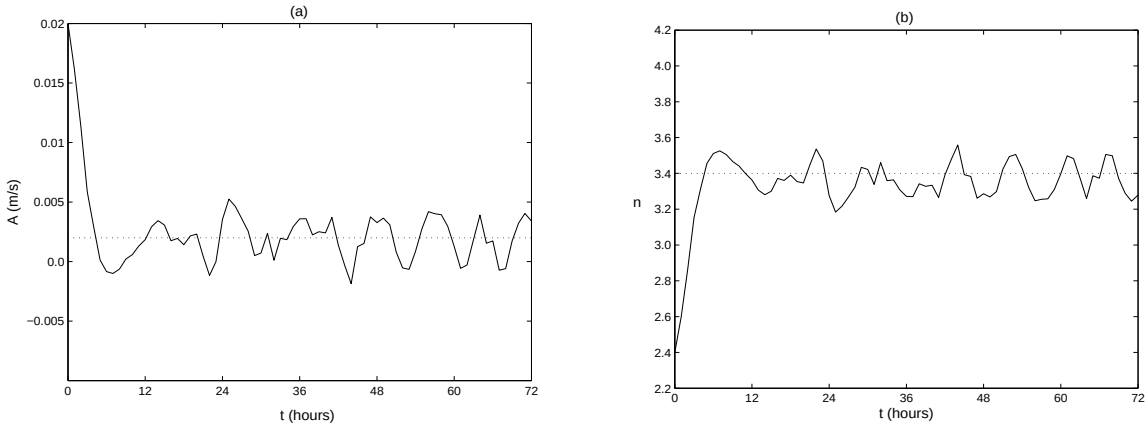

Figure 7.17: Underweighting the observations: true $\sigma_o = 0.1$, prescribed variances $\sigma_o^2 = 0.02$, $\sigma_b^2 = 0.01$, parameter updates for initial estimates $A_0 = 0.02\,\mathrm{ms}^{-1}$ and $n_0 = 2.4$.

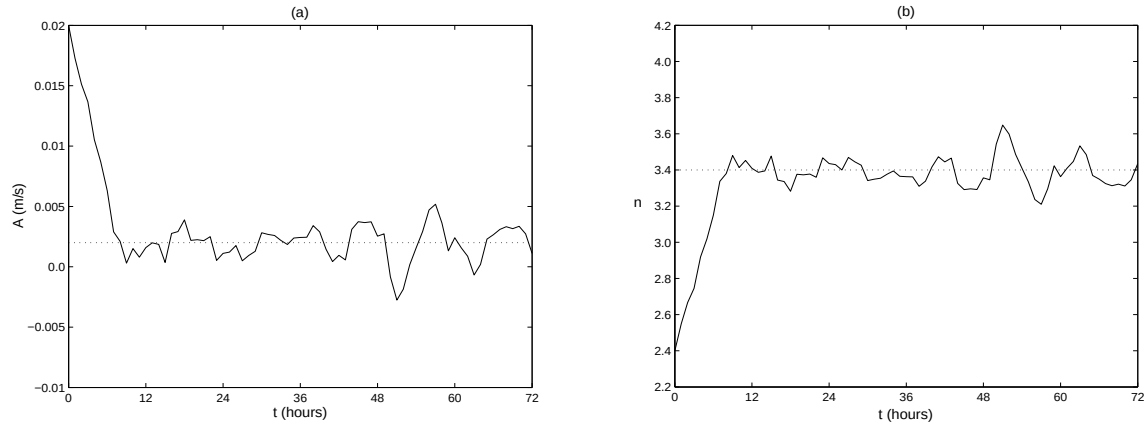

Figure 7.18: Underweighting the observations: true $\sigma_o = 0.1$, prescribed variances $\sigma_o^2 = 0.05$, $\sigma_b^2 = 0.05$, parameter updates for initial estimates $A_0 = 0.02\,\mathrm{ms}^{-1}$ and $n_0 = 2.4$.

8 Conclusions

We have been investigating the application of data assimilation techniques to the problem of morphodynamic model parameter estimation with particular focus on the role of the background error covariance matrix. This matrix plays an important role in the filtering and spreading of observational data. For parameter estimation, it is vital that the cross-covariances between the parameters and the state are given a good a priori specification as it is these covariances that that pass information from the observed variables to improve the estimates of the unobserved parameters. Our previous work (Smith et al. (2008), Smith et al. (2009)) found that a flow dependent specification of this matrix is needed for accurate parameter updating. However, explicitly propagating the error covariances would be computationally expensive and require the construction of adjoint and tangent linear models. In this report we have proposed a new hybrid approach. By combining the 3D Var and Kalman filter techniques we have developed a scheme that provides a flow dependent approximation of the state-parameter cross-covariances but which avoids the computational complexities associated with implementation of the full Kalman filter method.

This new method has been tested using an idealised, 1D non-linear sediment transport model that has two uncertain parameters. The results are positive with the scheme able to recover the model parameters to a good level of accuracy. This has a direct impact on the model; the model becomes a much better representation of the truth and thus produces more accurate forecasts of the future bathymetry. These results suggests that there is great potential for the use of data assimilation based morphodynamic model parameter estimation.

In our model, the number of parameters is small and therefore the increase in the dimension of the problem caused by the addition of the parameters to the state vector does not have a significant impact on computational cost. The finite difference calculation used in the approximation of the state-parameter cross covariance is therefore feasible. This could, however, potentially become an issue if state vector and/or the number of parameters to be estimated is large.

A particular issue encountered during this work was that, in addition to the state-parameter cross covariances being correctly specified, it is also important that that parameter error covariances (as described by the matrix $\mathbf{B_{pp}}$) are consistent with the true error statistics. We found that there was a strong correlation between the parameters A and n (caused by the formulation of the model). The values assigned to the parameter error variances σ_A^2 and σ_n^2 and covariance σ_{An} therefore had a significant affect on the accuracy of the estimates obtained. In particular it was crucial that the sign of σ_{An} was correctly chosen. This would perhaps be less important for a model whose parameters were less correlated and more easily identifiable. In practical situations, where the true statistics of the errors are not known, a model sensitivity analysis could be used to help identify the interdependence of parameters and ascertain whether cross correlations are needed. In some situations, it may even be prudent to consider a re-parameterisation of the model equations to improve the identifiability of the parameters. Another possible approach is to transform the parameters to a set of uncorrelated variables (Sorooshian and Gupta (1995)).

We eventually intend to use data assimilation for parameter estimation in a full morphodynamic assimilation-forecast system applied to some real coastal study sites. An obvious and useful extension to the current work would be to confirm our belief that the methodology presented here is transferrable by testing the approach in a second toy model.

A Tangent Linear Model (TLM)

Definition

If $\mathbf{f}$ is a non linear model defined as

$$\mathbf{z}_{k+1} = \mathbf{f}(\mathbf{z}_k),$$

then the *tangent linear model* of $\mathbf{f}$, called $\mathbf{F}$ is

$$\boldsymbol{\delta}\mathbf{z}_{k+1} = \mathbf{F}_k \boldsymbol{\delta}\mathbf{z}_k = \frac{\partial \mathbf{f}(\mathbf{z}_k)}{\partial \mathbf{z}} \boldsymbol{\delta}\mathbf{z}_k$$

Tangent Linear of the augmented system model

Starting from an initial state $\widehat{\mathbf{w}}_k$ at time t_k we generate a reference state at t_{k+1} using the model equation (2.4)

$$\widehat{\mathbf{w}}_{k+1} = \tilde{\mathbf{f}}(\widehat{\mathbf{w}}_k). \tag{A.1}$$

We define a perturbation to this state as

$$\boldsymbol{\delta}\mathbf{w}_{k+1} = \mathbf{w}_{k+1} - \widehat{\mathbf{w}}_{k+1}. \tag{A.2}$$

This perturbation then satisfies

$$\boldsymbol{\delta}\mathbf{w}_{k+1} = \tilde{\mathbf{f}}(\mathbf{w}_k) - \tilde{\mathbf{f}}(\widehat{\mathbf{w}}_k). \tag{A.3}$$

Assuming $\boldsymbol{\delta}\mathbf{w}_{k+1}$ is small, we can expand (A.3) in a Taylor series about $\widehat{\mathbf{w}}_{k+1}$. To first order we have

$$\begin{aligned} \boldsymbol{\delta}\mathbf{w}_{k+1} &= \tilde{\mathbf{f}}(\widehat{\mathbf{w}}_k + \boldsymbol{\delta}\mathbf{w}_k) - \tilde{\mathbf{f}}(\widehat{\mathbf{w}}_k) \\ &= \tilde{\mathbf{f}}(\widehat{\mathbf{w}}_k) + \mathbf{F}_k\boldsymbol{\delta}\mathbf{w}_k + \ldots - \tilde{\mathbf{f}}(\widehat{\mathbf{w}}_k) \\ &\approx \mathbf{F}_k\boldsymbol{\delta}\mathbf{w}_k, \end{aligned} \tag{A.4}$$

where

$$\mathbf{F}_k = \frac{\partial\tilde{\mathbf{f}}(\widehat{\mathbf{w}}_k)}{\partial\mathbf{w}}, \tag{A.5}$$

is the Jacobian of the forecast model with respect to $\mathbf{w}$ evaluated at $\widehat{\mathbf{w}}_k$.

Thus we can approximate

$$\tilde{\mathbf{f}}_k(\mathbf{w}_k) - \tilde{\mathbf{f}}_k(\widehat{\mathbf{w}}_k) \approx \mathbf{F}_k(\mathbf{w}_k - \widehat{\mathbf{w}}_k) \tag{A.6}$$

Note that this approximation is only valid if the perturbations to the model state are small, i.e. small $\|\mathbf{w} - \widehat{\mathbf{w}}_k\|_2$

Acknowledgements This work is funded under the UK Natural Environmental Research Council (NERC) Flood Risk From Extreme Events (FREE) programme, with additional funding provided by the Environment Agency as part of the CASE (Co-operative Awards in Science and Engineering) scheme. We would like to thank Dr Tania Scott and Professor Mike Baines for useful discussions.

References

Barnett, S. and Cameron, R. (1990). *Introduction to Mathematical Control Theory*. Oxford Applied Mathematics and Computing Science Series. Oxford Clarendon Press, second edition.

Bell, M., Martin, M., and Nichols, N. (2004). Assimilation of data into an ocean model with systematic errors near the equator. *Quarterly Journal of the Royal Meteorological Society*, 130:873–894.

Courtier, P., Andersson, E., Heckley, W., Pailleux, J., Vasiljevic, D., Hamrud, M., Hollingsworth, A., Rabier, F., and Fisher, M. (1998). The ECMWF implementation of three-dimensional variational assimilation (3D-Var). I: Formulation. *Quarterly Journal of the Royal Meteorological Society*, 124:1783–1807.

Dee, D. P. (2005). Bias and data assimilation. *Quarterly Journal of the Royal Meteorological Society*, 131:3323–2243.

Evensen, G. (1994). Sequential data assimilation with a nonlinear quasi-geostrophic model using monte carlo methods to forecast error statistics. *Journal of Geophysical Research*, 99(C5):10143–10162.

Evensen, G., Dee, D. P., and Schröter, J. (1998). Parameter estimation in dynamical models. In Chassignet, E. and Verron, J., editors, *Ocean Modeling and Parameterization*, pages 373–398. Kluwer Academic Publishers.

Fisher, M. (1998). Development of a simplified kalman filter. Technical Memorandum No. 260, ECMWF Research Department.

Gelb, A. (1974). *Applied Optimal Estimation*. M.I.T Press.

Gill, P. E., Murray, W., and Wright, M. H. (1981). *Practical Optimization*. Academic Press.

Grass, A. (1981). Sediment transport by waves and currents. Report No: FL29, SERC London Centre for Marine Technology.

Griffith, A. K. and Nichols, N. K. (1996). Accounting for model error in data assimilation using adjoint methods. In Berz, M., Bischof, C., Corliss, G., and Griewank, A., editors, *Computational Differentiation: Techniques, Applications and Tools*, pages 195–204. SIAM Philadelphia.

Griffith, A. K. and Nichols, N. K. (2000). Adjoint techniques in data assimilation for treating systematic model error. *Journal of Flow, Turbulence and Combustion*, 65:469–488.

Hill, D., Jones, S., and Prandle, D. (2003). Derivation of sediment resuspension rates from accoustic backscatter time-series in tidal waters. *Continental Shelf Research*, 23:19–40.

Houtekamer, P. and Mitchell, H. L. (2005). Ensemble Kalman filtering. *Quarterly Journal of the Royal Meteorological Society*, 131:3269–3289.

Ide, K., Courtier, P., Ghil, M., and Lorenc, A. (1997). Unified notation for data assimilation: Operational, sequential and variational. *Journal of the Meteorological Society of Japan*, 75(1B):181–189.

Jazwinski, A. H. (1970). *Stochastic Processes and Filtering Theory*. Academic Press.

Kalman, R. (1960). A new approach to linear filtering and prediction problems. *Transactions of the ASME - Journal of Basic Engineering (Series D)*, 82:35–45.

Kalman, R. and Bucy, R. (1961). New results in linear filtering and prediction theory. *Transactions of the ASME - Journal of Basic Engineering (Series D)*, 83:95–108.

Knaapen, M. and Hulscher, S. (2003). Use of genetic algorithm to improve prediction of alternate bar dynamics. *Water Resources Research*, 39(9):1231.

Lesser, G., Roelvink, J., van Kester, J., and Stelling, G. (2004). Development and validation of a three-dimensional morphological model. *Coastal Engineering*, 51:883–915.

Lewis, J. M., Lakshmivarahan, S., and Dhall, S. (2006). *Dynamic Data Assimilation: A Least Squares Approach*, volume 104 of *Encyclopedia of Mathematics and its applications*. Cambridge University Press.

Lorenc, A. (1981). A global three-dimensional multivariate statistical interpolation scheme. *Monthly Weather Review*, 109:701–721.

Martin, M., Bell, M., and Nichols, N. (2002). Estimation of systematic error in an equatorial ocean model using data assimilation. *International Journal for Numerical Methods in Fluids*, 40:435–444.

Martin, M., Nichols, N., and Bell, M. (1999). Treatment of systematic errors in sequential data assimilation. Technical Note No. 21, Meteorological Office, Ocean Applications Division.

Martin, M. J. (2000). *Data Assimilation in Ocean Circulation Models with Systematic Errors*. PhD thesis, University of Reading. Available at http://www.reading.ac.uk/maths/research/.

Mason, D., Davenport, I., Flather, R., Gurney, C., Robinson, G., and Smith, J. (2001). A sensitivity analysis of the waterline method of constructing a digital elevation model for intertidal areas in an ers sar scene of eastern england. *Estuarine, Coastal and Shelf Science*, 53:759–778.

Masselink, G. and Hughes, M. G. (2003). *Introduction to Coastal Processes and Geomorphology*. Hodder Arnold.

Navon, I. M. (1997). Practical and theoretical aspects of adjoint parameter estimation and identifiability in meteorology and oceanography. *Dynamics of Atmosphere and Oceans*, 27:55–79.

Pinto, L., Andre, B., and Fortunato, P. F. (2006). Sensitivity analysis of non-cohesive sediment transport formulae. *Continental Shelf Research*, 26:1826–1839.

Rodgers, C. D. (2000). *Inverse Methods for Atmospheric Sounding: Theory and Practice*, volume 2 of *Series on Atmospheric, Oceanic and Planetary Physics*. World Scientific.

Ruessink, B. (2005). Predictive uncertainity of a nearshore bed evolution model. *Continental Shelf Research*, 25:1053–1069.

Scott, T. R. and Mason, D. C. (2007). Data assimilation for a coastal area morphodynamic model: Morecambe Bay. *Coastal Engineering*, 54:91–109.

Smith, P. J., Baines, M. J., Dance, S. L., Nichols, N. K., and Scott, T. R. (2007). Simple models of changing bathymetry with data assimilation. Numerical Analysis Report 10/2007, Department of Mathematics, University of Reading. Available at http://www.reading.ac.uk/maths/research/.

Smith, P. J., Baines, M. J., Dance, S. L., Nichols, N. K., and Scott, T. R. (2008). Data assimilation for parameter estimation with application to a simple morphodynamic model. Mathematics Report 2/2008, Department of Mathematics, University of Reading. Available at http://www.reading.ac.uk/maths/research/.

Smith, P. J., Baines, M. J., Dance, S. L., Nichols, N. K., and Scott, T. R. (2009). Variational data assimilation for parameter estimation: application to a simple morphodynamic model. *Ocean Dynamics*.

Sorooshian, S. and Gupta, V. (1995). Model calibration. In Singh, V., editor, *Computer models of watershed hydrology*, chapter 2, pages 23–68. Water Resources Publications, Colorado.

Soulsby, R. (1997). *Dynamics of marine sands*. Thomas Telford Publications.

Spiegelman, M. and Katz, R. F. (2006). A semi-lagrangian crank-nicolson algorithm for the numerical solution of advection-diffusion problems. *Geochemistry Geophysics Geosystems*, 7(4).

Trudinger, C., Raupach, M., Rayner, P., and Enting, I. (2008). Using the kalman filter for parameter estimation in biogeochemical models. *Environmetrics*, 19(8):849–870.

van Dongeren, A., Plant, N., Cohen, A., Roelvink, D., Haller, M. C., and Catalán, P. (2008). Beach Wizard: Nearshore bathymetry estimation through assimilation of model computations and remote observations. *Coastal Engineering*. In press.

van Rijn, L. C. (1993). *Principles of Sediment Transport in Rivers, Estuaries and Coastal Seas*. Aqua Publications.

Vrugt, J., Diks, C., Gupta, H., Bouten, W., and Verstraten, J. (2005). Improved treatment of uncertainity in hydrologic modeling: Combining the strengths of global optimization and data assimilation. *Water Resources Research*, 41(1). W01017.

Wüst, J. (2004). Data-driven probablistic predictions of sand wave bathymetry. In S.J.M.H., H., Garlan, T., and Idier, D., editors, *Marine Sandwave and River Dune Dynamics II*. Proceedings of International Workshop, University of Twente.